

STRATOSPHERIC OZONE INTERCOMPARISON CAMPAIGN (STOIC) 1989: OVERVIEW

J. J. Margitan¹, R. A. Barnes², G. B. Brothers², J. Butler³, J. Burris⁴, B. J. Connor⁵, R. A. Ferrare⁶, J. B. Kerr⁷, W. D. Komhyr⁸, M. P. McCormick, I. S. McDermid¹, C. T. McElroy⁷, T. J. McGee⁴, A. J. Miller⁹, M. Owens¹⁰, A. D. Parrish¹¹, C. L. Parsons¹², A. L. Torres¹², J. J. Tsou¹³, T. D. Walsh¹, D. Whiteman¹⁴

August 1994

1 Jet Propulsion Laboratory, California Institute of Technology, Pasadena, CA

2 Chemal, Inc, Wallops Island, VA (now at ManTech, Wallops island, VA)

3 Hughes STX Corporation, Lanham, MD

4 Laboratory for Atmospheres, NASA /GSFC, Greenbelt, MD

5 Atmospheric Sciences Division, NASA /LaRC, Hampton, VA

6 Universities Space Research Association, NASA/GSFC, Greenbelt, MD (now at Hughes STX Corporation, Lanham, MD)

7 Atmospheric Environment Service, Downsview, Ontario, Canada

8 NOAA Climate Monitoring and Diagnostics Laboratory (formerly Geophysical Monitoring for Climate Change), Boulder, CO (now at CIRES, Univ. Colorado, Boulder, CO)

9 NOAA Climate Analysis Center, Washington, DC

10 Department of Physics, University of Maryland, College Park, MD

11 Department of Physics and Astronomy, University of Massachusetts, Amherst, MA

12 Wallops Flight Facility, NASA/GSFC, Wallops Island, VA

13 Lockheed Engineering and Sciences Co., Hampton, VA

14 Laboratory for Terrestrial Physics, NASA /GSFC, Greenbelt, MD

STRATOSPHERIC OZONE INTERCOMPARISON CAMPAIGN (STOIC) 1989: OVERVIEW

ABSTRACT

The NASA Upper Atmosphere Research Program organized a Stratospheric Ozone Intercomparison Campaign (STOIC) held in July-August 1989 at the Table Mountain Facility (TMF) of the Jet Propulsion Laboratory. Participating in this campaign were several instruments that had been recently developed by NASA for the Network for the Detection of Stratospheric Change: the JPL ozone lidar at TMF, the GSFC trailer-mounted ozone lidar which was moved to TMF for this comparison, and the Millitech/LaRC microwave radiometer.

In order to assess the performance of these new instruments, a validation /intercomparison campaign was undertaken using established techniques: balloon ozonesondes launched by personnel from the Wallops Flight Facility and from NOAA GMCC (now CMDL), a NOAA GMCC Dobson, and a Brewer from the Atmospheric Environment Service of Canada, both being used for column as well as Umkehr profile retrievals. All of these instruments were located at TMF and measurements were made as close together in time as possible to minimize atmospheric variability as a factor in the comparisons. Daytime rocket measurements of ozone were made by WFF personnel using ROCOZ-A instruments launched from San Nicholas Island. The entire campaign was conducted as a blind intercomparison, with the investigators not seeing each others data until all data had been archived at the end of the two week period (July 20- August 2). Satellite data were also obtained from the Stratosphere Aerosol and Gas Experiment (SAGE 11) aboard the Earth Radiation Budget Satellite and the Total Ozone Mapping Spectrometer (TOMS) aboard Nimbus-7.

An examination of the data has found excellent agreement among the techniques, especially in the 20-40 km range. As expected, there was little atmospheric variability during the intercomparison, allowing for detailed statistical comparisons at a high level of precision. This overview paper will summarize the campaign and provide a "roadmap" to subsequent papers in this issue by the individual instrument teams which will present more detailed analysis of the data and conclusions.

INTRODUCTION

Measurement of the abundance of ozone in the Earth's stratosphere and its susceptibility to modification due to a variety of natural and anthropogenic causes has been a central focus of atmospheric research for decades. As the only significant atmospheric absorber of near UV solar radiation, ozone abundance not only controls the flux of solar UV at ground level, but also plays a major role in creating the temperature structure of the stratosphere. In the past two decades we have seen a dramatic improvement in our knowledge of the processes controlling stratospheric ozone, now recognizing that the simple production of ozone from solar photodissociation of molecular oxygen is balanced by a series of catalytic destruction processes involving the odd hydrogen, nitrogen and chlorine families. While these species exist as a consequence of natural sources of precursor trace gases in the lower atmosphere, we now recognize that mankind has the capability to significantly increase source gas emissions, and consequently change in significant ways, the ozone destruction processes. Concerns in the past decades have centered on emissions from supersonic transports, space shuttle and rockets, degradation of fertilizer, increased biological activity/productivity, and perhaps best known, emissions of chlorine and bromine compounds (chlorofluorocarbons, Halons, and other halocarbons). The localized, seasonal Antarctic ozone hole provides highly visible evidence of the susceptibility of ozone to destruction; the much smaller global decrease inferred from longer term datasets demonstrates the pervasive extent of ozone decline (WMO, 1985, 1988, 1991).

The existence of ozone over a wide range of concentrations and atmospheric altitudes and pressures has led to the development of a wide

variety of techniques for measuring it utilizing rocket, balloon, ground and satellite platforms on a variety of spatial and temporal integration scales, The wide variety of available ozone measuring techniques is also coupled to the evolution from necessarily localized measurements many decades ago to the global coverage afforded by satellites today. Although space-borne techniques are clearly the only way of obtaining global ozone measurements, the desire to identify very small (few percent) changes in ozone over long time scales (decades) requires that the satellite sensors not be used in isolation. Rather, ongoing campaigns of ground-truth and intercomparison are needed, not only to provide an assessment of the strengths and weaknesses of the various techniques, but also to provide a means of comparing data sets obtained by different instruments at different times.

Toward this end, a number of intercomparison campaigns have been conducted for ozone measuring instruments (see WMO 1985 for a summary), including the Ozone Intercomparison Campaign in 1981, the Balloon Ozone Intercomparison Campaign (BOIC) in 1983-1984 (*Hilsenrath et al.*, 1986), and the Balloon Intercomparison Campaign (BIC) in 1982-1983. A particularly gratifying result of these campaigns was that it does indeed appear that it is possible to make ozone measurements in the stratosphere within an accuracy of a few percent over an altitude range from 15-40 km.

In the past few years, a number of new instruments have been developed specifically for the role of identifying long term trends in stratospheric composition. In addition to their role in the international Network for the Detection of Stratospheric Change, these instruments would also provide a crucial validation/long term calibration standard for satellite sensors such as SBUV/2 aboard the NOAA weather satellites and the various instruments aboard the Upper Atmosphere Research Satellite, UARS

(CLAES, MLS, HALOE, ISAMS). Although these new instruments promise significantly improved capability over many of the older techniques, the existence of the long term database from those older instruments makes it mandatory that a detailed intercomparison campaign be carried out to assess the relative performance and to provide a means to interrelate the various datasets.

In order to carry out this comparison, the Stratospheric Ozone Intercomparison Campaign (STOIC) was conducted for a two week period in July-August 1989 at the Jet Propulsion Laboratory's Table Mountain Facility (TMF) near Pasadena, CA. The participating instruments are shown in Table 1, along with their observing location and observing times. The timing of the campaign was chosen to minimize atmospheric variability as a factor as well as to allow for the maximum opportunity for observations and satellite coincidences. To further minimize atmospheric variability, the instruments were, to the extent practical, colocated at TMF, and observations were made as close together in time as possible. Subsequent analysis of the results (see later) demonstrates that this objective was achieved. For this campaign, the altitude region of interest was 20-50 km, although some instruments have performance capabilities beyond that range.

A very significant aspect of this intercomparison was the adherence to a data protocol to ensure that the various instrument results were "blind". For the entire two week period, no investigator saw the results of any other investigator, and each day's results were turned in to an independent coordinator. Investigators followed their standard data analysis procedures. Investigators were free throughout the period to revise their initial blind results based on performance information obtained from their own instrument as the campaign progressed, leading to a final set of "blind" data

for comparison. After the end of the two week comparison period, these blind results were studied. As will be discussed later, they are in excellent agreement. Nonetheless, they do highlight some specific instrument problems and discrepancies, sometimes as simple as data analysis software bugs. Based on these blind comparisons, some teams did reanalyze their data to generate "revised" datasets. These revisions, fully discussed in this sequence of papers, led to a second set of revised comparisons. The bottom line conclusion from the STOIC series is that the newly developed instruments of the NDSC have the capability to perform measurements at accuracies approaching 5% over the critical 20-40 km altitude range, with uncertainties increasing to greater than 10% by 50 km.

INSTRUMENTS

The participating instruments listed in Table 1 are briefly described in following subsections. The main site for the campaign was TMF at an altitude of 7500 ft. (2300 m) in the San Gabriel Mountains north of Los Angeles (34.4 N, 117.7 W). The JPL lidar had been operating at TMF for some time prior to this campaign. The GSFC trailer mounted lidar had previously been at TMF and returned for STOIC. Both are excimer laser based systems. The 110 GHz microwave instrument was newly installed at TMF. These three instruments were the newly developed ones for the NDSC. The microwave radiometer has the capability of making both day and night measurements of ozone. The lidars could only be operated at night, and had to be operated sequentially to avoid interference.

For comparison with these instruments, rocket ozonesondes (ROCOZ-A) were launched by personnel from the Wallops Flight Facility (WFF) at the US Navy site on San Nicholas Island, approximately 100 miles west of TMF. Balloon ozonesondes (ECC) were launched by WFF personnel at both Pt. Mugu (supporting San Nicholas) and TMF, using their standard procedures. Personnel from the NOAA CMDL (Climate Monitoring and Diagnostics Laboratory, formerly Geophysical Monitoring for Climate Change, GMCC) also launched ECC sondes from TMF using their own, slightly different, procedures. Both groups launched at night during the lidar observations. The NOAA group also operated a Dobson instrument at TMF for both column and profile data (the latter using the Umkehr technique). Additionally, a Brewer spectrometer from AES/Canada was operated at TMF, also performing column and (Umkehr) profile measurements. Satellite observations were made by the SAGE II instrument on ERBS on a number of

overpasses, and column data were obtained from the TOMS instrument aboard Nimbus 7. Meteorological data were provided by NOAA CAC (Climate Analysis Center). The *in situ* UV Photometers that performed so well in BOIC could not be flown for this campaign due to the lack of suitable landing areas in the heavily populated Southern California region. A ground based Dasibi was also used for measuring surface ozone abundance, which although not directly relevant to the STOIC measurements, is of value in understanding diurnal and day-to-day changes in the column amount. The surface measurements are not discussed further here, but are presented in McDermid and Walsh (this issue).

The operating altitude ranges and dates of operation for the instruments are shown in Figure 1 and Table 2. Table 3 contains precision and accuracy information for the individual instruments at a variety of altitudes. These performance claims are those of the individual investigators, and no attempt to critically evaluate them by the STOIC team was made. The individual instrument papers should be consulted for the basis of the figures,

Brief Descriptions of the STOIC Instruments:

GSFC Stratospheric Ozone Lidar The GSFC lidar is a mobile system mounted in a 45 foot long trailer. The instrument transmitted two laser wavelengths: 307.9 nm generated by a line-narrowed XeCl laser, and 355 nm, the third harmonic of a Nd:YAG laser. Backscattered light, at the transmitted wavelengths, was collected using a 30 inch telescope, separated by dichroic optics, and detected by photomultiplier tubes in a photon counting mode. Two detectors were used for each transmitted wavelength to increase the dynamic range of the lidar. Differential absorption provides the basis for the

extraction of an ozone profile from the backscattered returns. Ozone absorbs at 307.9 nm and is much less absorbent at 355 nm (about 3 orders of magnitude less). Therefore an analysis of the difference in slope between returns at the two wavelengths results in a vertical profile of ozone. Because of the small difference in absorption at high altitudes where the concentration is small, it is necessary to integrate the returns for approximately 4 hours to achieve the necessary signal to noise. This amounts to 106 shots at 307.9 nm and 2.5×10^5 at 355 nm. Temperature is also extracted from the 355 nm return. Because of interference from Mie scattering, the temperature profile is limited to a lower altitude of 30 km. During STOIC, temperatures were retrieved to an altitude above 70 km (*Ferrare et al.*, this issue). The GSFC lidar has been discussed in detail in a previous publication (*McGee et al.*, 1991).

JPL Stratospheric Ozone Differential Absorption Lidar. Complete details of the JPL-TMF differential absorption lidar system and the data analysis procedures have been published elsewhere [*McDermid and Godin*, 1989; *McDermid et al.*, 1990a, b]. Briefly, a high-power (100 W), narrow-bandwidth, tunable, xenon chloride (XeCl) excimer laser system provides directly the absorbed, probe wavelength at 307.9 nm. The reference wavelength, 353.2 nm, is generated by stimulated Raman shifting of a portion of the fundamental beam in a high pressure (400 psig) hydrogen cell. Thus, the two wavelengths are transmitted simultaneously in time and, by careful alignment, in space. The radiation backscattered by the atmosphere is collected with a 90-cm-diameter telescope and the two wavelengths are separated by a series of dichroic beamsplitters and interference filters. The signal is then measured using photomultipliers and photon counting techniques. The system operates only at night and the signal is averaged for 106 laser pulses, which takes

approximately 2 hours, to derive a single stratospheric ozone profile, The ozone number density is obtained from the difference of the derivatives of the signals recorded for each wavelength, divided by the ozone differential absorption cross section, taking into account the temperature dependence of this cross section, and the wavelength dependence of the Rayleigh backscatter and extinction. The slope (derivative) of the background corrected signal is computed as a function of range, As the altitude is increased, the range resolution of the measurement has to be degraded to limit the increase in the statistical error related to the rapid decrease in the signal level (see table 3). In this particular lidar implementation the largest source of error has been found to be associated with the determination of the background signal.

Millitech/LaRC Microwave The microwave instrument is intended for long term ozone monitoring, and is largely automated so that it requires a minimum of operator attention. It was developed at the Millitech Corporation. The data calibration and retrieval algorithms used with the instrument were developed at the NASA Langley Research Center. The instrument consists of a microwave receiver and a 122 channel spectrometer. It was tuned to observe the ozone line at 110.836 GHz ($\lambda = 2.6$ mm) for all data reported in this paper, The receiver converts signals at its input to lower “intermediate” frequencies that can be processed by conventional electronic techniques in the filter spectrometer. The spectrometer’s filters are followed by detectors; the detectors outputs are digitized, integrated, and stored in the system computer. The instrument is calibrated using the thermal radiation from blackbody standards. The instrument, observing technique, and calibration method are described in Parrish, et al., 1992. The ozone altitude distribution is retrieved from the details of the pressure broadened line shape.

The retrieval method is described in Parrish, et al., 1992 and a detailed characterization of the results is presented in Connor et al. (this issue); it is based on the work of Rodgers (1976).

ECC ozonesondes. The ECC ozonesonde, a compact, lightweight, balloon-borne instrument, employs a wet-chemical method involving the reaction of ozone with potassium-iodide (KI) to measure the vertical distribution of ozone. The sensor is made of two bright-platinum electrodes immersed in KI solutions of different concentrations contained in separate cathode and anode chambers linked together with an ion bridge. Driving e.m.f. for sensor operation is provided by the different solution concentrations. Ozone in air, forced into the sensor cathode by a non-reactive gas sampling pump during balloon ascent, reacts with the aqueous KI solution to form iodine (I_2). The sensor then reconverts the I_2 to iodide, at which time two electrons flow in the sensor's external circuit corresponding to each molecule of ozone entering the sensor. A measure of the sensor's output current translates, therefore, into the rate of ozone entry into the sensor per unit time. During balloon ascent the ECC instrument is connected to a meteorological radiosonde for ozone data transmission to a ground receiving station. Transmitted data include air pressure, temperature, and relative humidity. See Komhyr et al. (this issue) for more details.

ECC ozonesondes flown during STOIC by NOAA and WFF personnel were essentially identical, but operating procedures were different in some respects. These differences are traditional between the two institutions, and were maintained here, rather than imposing a uniform procedure. ECC sensor cathode KI solutions in the WFF instruments were slightly more concentrated (by 0.5%), causing a small difference in the stoichiometry of the

KI-O₃ reactions in the NOAA and WFF sondes. Somewhat different pump efficiency corrections were used by the two groups at balloon flight altitudes above about 100 mb. NOAA ECC sonde ozone profiles were normalized to Dobson spectrophotometer total ozone, while the WFF instruments were calibrated prior to flight with an ozone source of known concentration, with calibration traceable to NIST. Finally, the NOAA sonde data were processed automatically during flight, while the WFF data were manually extracted from radiosonde receiver recorder charts for processing.

Dobson Spectrophotometer. The Dobson spectrophotometer is a UV double monochromoter capable of highly accurate measurements of the relative intensities of the double pair wavelengths A (305.5 /325.0 nm), B (308.9 /329.1 nm), C(311.5/332.4 nm), and D (317.5 /339.9 nm) emanating from the sun, moon, or zenith sky. The short wavelength of each pair is highly absorbed by ozone, while absorption at the longer wavelengths is only slight. Effective band passes are 1 nm for the short wavelength and 3 nm for the long wavelength of each pair. Total ozone amounts deduced from direct sun measurements are most accurate and can be made on any of the wavelength pairs, taking into account the solar elevation at the time of observation, relevant ozone absorption coefficients, and light scattering by air molecules and aerosols. To eliminate aerosol interference which is difficult to quantify, observations are made on double pair wavelengths such as the fundamental AD wavelengths. Aerosol effects are eliminated through a subtraction process since aerosol scattering is highly similar for the A and D wavelengths. All Dobson spectrophotometers in use throughout the world are calibrated periodically relative to World Standard Dobson Spectrophotometer No. 83, whose long term ozone measurement precision has been maintained at $\pm 1\%$

since 1962 (*Komhyr et al.*, 1989). Ozone measurement precision for the instrument is $\pm 0.3\%$, and ozone measurement accuracy is estimated to be $\pm 3.0\%$.

During STOIC, ozone vertical profiles (*Komhyr et al.*, this issue) were also made with the Dobson instrument employing the Umkehr technique (*Gotz et al.*, 1934; *Mateer and Dutsch*, 1964; *Mateer and DeLuisi*, 1992). Umkehr observations are made in mornings or afternoons on light scattered from the clear zenith sky. The measurements are based on the principle that the effective scattering height in the atmosphere for any of the Dobson instrument pairs, e. g., C, varies during times of rising or setting sun.

Brewer Spectrophotometer. The automated Brewer Ozone Spectrophotometer was developed during 1979-81 at the Atmospheric Environment Service (AES) in Canada for the purpose of measuring column ozone operationally with the high stability necessary for accurate long-term trend analysis. It is a modified Ebert grating spectrophotometer which can be programmed to sequence automatically measurements of total ozone (using the direct sun, zenith sky or focussed moon measurement method), the ozone profile using the Umkehr method, and UV-B radiation. The World Meteorological Organization Brewer instrument #39 was used during STOIC to measure total ozone using the direct sun method (*Kerr and McElroy*, this issue) and the ozone profile using the Umkehr method (*McElroy and Kerr*, this issue). The instrument and the methods to measure total ozone are described by Kerr et al. (1983, 1985) and Evans et al. (1987), and the Umkehr method for ozone profiles by Mateer et al. (1985) and McElroy et al. (1989, 1990, this issue).

ROCOZ-A. The improved Rocket Ozonesonde (ROCOZ-A) is launched aboard a Super-Loki booster to approximately 70 km, where the payload is ejected for parachute descent. The radiometer measures the solar UV irradiance over its filter wavelengths as it descends through the atmosphere. The amount of ozone in the path between the radiometer and the sun is then calculated from the attenuation of solar flux as the instrument falls. In addition, radar from the launch site measures the height of the payload throughout its descent, which, combined with knowledge of the solar zenith angle allows calculation of the overhead ozone column as a function of geometric altitude. Ozone mixing ratio can be calculated as the derivative of the column amount with respect to pressure. The ROCOZ-A and its performance are described more fully in Barnes et al. (1989).

RESULTS AND DISCUSSION

Shown in Figure 2 are the "blind" results from a "sample," day, July 24, 1989, referred to as 890724 (in YYMMDD format), the day being UT. This was the only day in the two week period that had results from all instruments, due to the limited SAGE II overpass opportunities (3) and the limited ROCOZ launches (6). As can be seen from the linear and semilogarithmic presentations the results are in very good agreement. It is obvious from the profiles that the GSFC lidar falls off above -42 km, due to rapidly decreasing signal returns coupled with difficulties in treating signal-induced noise in the background region of the lidar return, a common problem for high-powered lidars not equipped with a shutter in front of the detectors. There was no uniform, fixed maximum altitude for cutoff; rather it varied from day to day in the blind submissions. A similar dramatic increase in uncertainty occurs in the JPL lidar for the same reason, albeit at a slightly higher altitude due to the increased laser power of the JPL system. Following an examination of the data at the end of the campaign, revisions were made to some instrument datasets, in the GSFC lidar case, for example, terminating the profile at the point at which the group could no longer have confidence in the measurement of ozone. Truncation was chosen as a better alternative than altering the background determination, which would have made the profiles agree at higher altitudes. These revised profiles are shown in Figure 3. For these profiles, as well as all others in this overview, the individual profiles were interpolated using a cubic spline function onto 0.5 km spacing to permit direct comparison.

Atmospheric variability has always been an issue that has hampered measurement intercomparisons. To minimize its effect here, the campaign

was carried out during the summer which is a period of reduced variability, and attempts were made to make measurements as close together in time and space as practical. One indication of the extent of atmospheric variability during this period is obtained in Figure 4a-d, which show the daily average profiles, obtained for each day by simply averaging the available measurements. Figure 5 shows the data as a contour plot. Since not all instruments measure ozone each day, and, as will be discussed later, there are some instrument-to-instrument variations, the variability shown in Figures 4 and 5 is slightly enhanced over the true atmospheric variability. Nonetheless, the conclusion from Figures 4 and 5 is that atmospheric variations during the daily measurement period were small.

Given the limited day-to-day variability during this period, it was appropriate to compute an average profile for each instrument, obtained from the individual days' data, even though not all instruments made measurements on all days. These instrument average profiles, for the blind data, are shown in Figure 6. It is clear from Figure 6, and from Figure 2, that the excellent agreement among the techniques makes it difficult to visualize the differences, when plotted in any usual manner. We therefore began comparing instruments to reference profiles and plotting the differences of the individual instruments from the reference. In order to try to keep the average difference near zero, it was most appropriate to compute internal STOIC references, rather than attempting to use some independent, external reference profile, which would have given rise to systematic offsets. This is not to imply that the STOIC measurements represent the "correct" atmospheric profile, although since these are purported to be among the best ozone measuring techniques, it should be very close. Any reference profile, computed by averaging the different measurements, will have errors in it

arising from contributions from the individual measurements. Thus, deviations of an individual measurement from the reference can not be construed as proof of a deficiency in that technique: even a “perfect” measurement will show differences from the reference since the reference was computed from “imperfect” data.

Several different approaches were taken to formulating reference profiles. First, the measurements for each day were averaged to obtain daily average profiles (the ones shown in Figure 4), and the individual measurements were then ratioed to that daily average, on a day-by-day basis. These differences were then plotted and examined. While this approach provides a wealth of useful data, it contains the flaw that the instruments contributing to a given day’s average change from day-to-day, and the individual instrument biases can cause the average to “shift” from day-to-day. To obtain a more consistent picture of instrument biases, all the available profiles from the two week period were averaged into a STOIC Reference Profile. This clearly does not give each instrument equal weight since each instrument had a different number of observations. It does, however, provide a single, consistent “normalization” profile against which all the individual profiles can be compared. The alternative technique of averaging the individual instrument averages led to a virtually identical profile.

This procedure was first carried out using the blind data, leading to the Blind STOIC Reference Profile. Comparisons of the individual profiles against this Blind Reference led to the identification of a number of instrumental problems. Some of these were as straightforward as, for example, discovering software “bugs” causing the first point in a profile to be artificially low. Identification of these problems allowed for the generation of revised datasets which could then all be averaged into a Revised STOIC

Reference Profile, which did not include such instrument artifacts. The individual blind profiles could then be better compared against this better, more correct, Revised Reference, It is this Revised Reference Profile that we refer to as the STOIC Reference Profile, The Blind and Revised instrument averages are compared to this STOIC Reference in Figure 7, plotted as $((\text{individual/reference}) - 1)$, so that 0.1 represents an instrument 10% higher, and -0.1 represents one 10% lower than the reference. These comparisons were carried out for the 20-50 km altitude range of interest. Since both the blind and revised comparisons in Figure 7 use the same reference, the small effect of revisions can be seen in that figure. The revisions that occurred for the individual instruments are discussed in detail in the individual papers of this issue, and are only briefly summarized here.

DATA REVISIONS

Eight of the twelve GSFC profiles were revised after an analysis of the data. In all cases, the revision consisted of a truncation of the profile at a lower altitude than previously reported. The truncation point was selected where the GSFC profile began to deviate systematically (always negatively) from the daily average. Below 40 km, the "blind" and "revised" profiles are identical. The reasons for this systematic error are discussed later.

Three significant features were noted in the comparison of the JPL-lidar blind profiles with the overall averages. First, at 45 km the comparison had an obvious inflection and the magnitude of the lidar deviation from the average started to increase rapidly. Second, there was a small but consistent difference, on the order of 5%, just above 30 km altitude where the high and low intensity profiles were joined together. Third, the very first point, at 20

km altitude, was always low by approximately 10%. These three points were carefully studied to see if there was a scientifically justifiable explanation and possible correction.

The problem identified at 20 km was caused by an error in the data analysis algorithm that incorrectly considered the raw data at lower altitudes in calculating the derivative of the signal at 20 km. This was readily corrected by starting the analysis calculations at a lower altitude.

The original rationale for using high and low intensity data to form a composite ozone profile was to avoid the need to apply a saturation correction to the raw data counts. It was apparent from the blind intercomparison that the high intensity data still showed a small degree of saturation immediately above the crossover point. There were two potential solutions to this problem. The first was to utilize the low intensity data up to a higher altitude where it was certain that the high intensity data were not saturated. This approach was rejected because the signal-to noise ratio of the low intensity data was falling rapidly and the errors in the ozone concentration would be increased significantly in this region. The second approach, which was adopted, was to apply a correction for saturation or pulse-pile-up caused by the finite dead-time of the photon counting system. This is described in detail in the paper by McDermid et al. in this issue.

At the upper end of the altitude range, the high intensity data, and in particular the 307.9 nm channel, have been seen to be affected by a signal-induced noise [McDermid et al, 1990a]. It has been determined that this is caused by the very high intensity of laser radiation backscattered from the boundary layer and the lower troposphere hitting the photocathodes of the photomultiplier detectors. This signal is not transmitted by the photomultiplier since it is electronically gated off during this time but the

dark current of the tube shows a delayed recovery [Lee *et al*, 1990]. The effect of this signal-induced noise is to increase and cause a curvature of the background level. Different methods of fitting the background have been studied [McDermid *et al*, 1990a; Iikura *et al*, 1987] and the best fit is given by a non-linear least-squares exponential regression. The ozone profile below -40-45 km is insensitive to the method used to estimate the background. However, above this altitude the profile is very sensitive to the background correction. For the non-linear exponential fit it is also found that the profile is sensitive to the starting altitude of the regression. An important factor in the background estimation is that the real signal must be negligible at the starting altitude but the fit must be started as low as possible in order to evaluate the curvature correctly. Various methods have been used to select the starting altitude and these were reconsidered in refining the data analysis. However, no suitable, justifiable modification could be identified. For the final refined results, the background fitting for the 307.9 nm high-intensity channel was started at 85 km for all data sets. The only improvement in the agreement of the results above 45 km was achieved by truncating some of the profiles. Based on consideration of the signal levels which were affected by clouds or other conditions some of the profiles were terminated at 47 km instead of 50 km.

Revisions to the microwave data were small, and were made only for 28 and 31 July. In both cases the GSFC lidar temperature profiles, which were used in processing the microwave data, were themselves revised subsequent to the campaign. The microwave data were then reprocessed using the new temperatures. Changes in the microwave ozone retrievals were between 2-4%. On 31 July, the revisions only affected altitudes above 50 km.

During the “blind” phase of STOIC, NOAA ECC sonde and Dobson total column data were processed on the Vigroux (1953, 1967) ozone absorption coefficient scale--a practice sanctioned by the International Ozone Commission. Because ozone measurements made with the other instruments during STOIC (except for the microwave instrument) were expressed on the newer Bass-Paur (1985) absorption coefficient scale, the NOAA values were reduced for compatibility by 3% to form the “revised” datasets. (More recently, Komhyr et al. (1993) have shown that the difference in the two scales is 2.6%; however, this 0.4% change has not been made to the data used here.)

There were some differences also in the “blind” and “revised” atmospheric pressures measured with the NOAA ECC sondes, primarily because of the newness of the NOAA automated sonde data acquisition system used at TMF, and inadequacy of the preliminary algorithm used for processing the radiosonde pressures. Changes made later to the algorithm allowed the pressures to be corrected.

The comparisons of the blind data provide an appraisal, for each technique, of the composite of the capability of that technique, the expertise of the particular group using it, and the maturity or evolution in the data analysis. From the standpoint of identifying the performance capability of the techniques for use in obtaining stratospheric ozone profiles, it is more valuable to concentrate on examining the comparisons of the revised data, which more clearly isolate the technique’s inherent capability from the operator’s capability. (The blind comparisons, however, provide an important indication of the potential limitations of using the data from an instrument obtained in an isolated setting.) The comparison of instrument

averages to the reference in Figure 7 leads to a number of obvious conclusions regarding the performance of the various instruments. These are discussed in greater detail in the accompanying individual papers, and only briefly here.

The most striking feature of Figure 7 is the excellent agreement among the techniques, measuring ozone within about $\pm 5\%$ over the 20-40 km region. In Figure 8, the standard deviations are shown, which also illustrates the little change between blind and revised data, the agreement among the techniques, and the decrease in performance above 40 km, arising from three sources: decreasing ozone abundance, decrease in available data, and rapid fall off in signal among the remaining lidar datasets. It seems reasonable to conclude, from Figures 7 and 8, that ozone measurements can be made to within $\pm 5\%$ over the 20-40 km region.

The consistent offset of the ROCOZ-A data by 5-10% high is also clear in Figure 7. While a 5% offset had been observed for ROCOZ during BOIC, no such offset was seen in a later comparison with SAGE II, or in the fall 1988 measurements preceding STOIC. The Barnes et al, paper (this issue) discusses ROCOZ performance in more detail,

The falloff in ECC sonde performance above 35 km is also apparent, not inconsistent with the results of prior campaigns such as BOIC. Both Barnes and Torres (this issue) and Komhyr et al (this issue) discuss ECC performance in greater detail.

The effect of the signal-induced noise problem and the resulting fall-off of the lidars at altitudes above about 40 km is apparent. Both of the GSFC and JPL lidars transmit high energy laser pulses into the atmosphere, to be detected after scattering from molecules in the atmosphere. In theory, then, a typical lidar return would fall off exponentially as the atmosphere thins, until

the magnitude of the scattered return is less than the background level of the detector. This background signal would be comprised of scattered moonlight, starlight, and the dark current of the photomultiplier tube. Because these signals are essentially constant on the time scale over which the lidar return is collected, this background region should therefore be flat. Subtraction of this flat background region from the recorded signal would yield an accurate measure of backscattered laser radiation. Actual recorded retruns, from both of the lidars in question, exhibit a background region which is not flat, but which slowly decays long after any expected scattered laser signal. The use of electronic gating on the PMT's reduces, but does not remove, this effect. An accurate determination of the background is extremely difficult under these conditions. The problem obviously becomes more important as the backscattered signal approaches the background (i. e., at high altitudes), This problem has been referred to as signal-induced noise, and appears to derive from the fact that a very large scattered laser return impinges on the photocathode of the PMT from low-altitude scattering of the transmitted laser pulse.

After much analysis, both lidar teams settled on an approach first suggested by McDermid and Godin. The background region is fit to an exponential function, If the fit converges, the function can then be extrapolated back into the altitude region which contains the scattered laser radiation. The solution of the function at each altitude is taken to be the "background" and is subtracted from the recorded signal. It is difficult, however, to know exactly at what altitude to begin the exponential fit to the background. The background fit, and subsequently, the ozone extraction at high altitudes, are very sensitive to this starting altitude. In order to make the selection of the starting altitude somewhat objective, the GSFC group

followed the routine developed by McDermid and Godin whereby a model lidar return for each of the transmitted wavelengths was constructed, Each day this model lidar return was normalized between 30 and 35 km to the actual lidar return recorded that day. The altitude at which the magnitude of the signal for this normalized model lidar return was equal to the noise on the actual lidar return between 100 and 200 km was selected as the starting altitude for the background fit. This arbitrary criterion appeared to yield “reasonable” results prior to the STOIC campaign. Subsequent analysis of the GSFC STOIC data indicated that on those days when a systematic negative bias was noted in the ozone profile above 40 km, lowering the starting altitude for the background fit would have brought the retrieved ozone more in line with the STOIC daily average.

For nights when there was a systematic deviation bias to the “blind” lidar data at high altitudes, there exist two possibilities for revising the data: truncation of the profile in question at the point where the profile becomes sensitive to the background fit, or adjustment to the starting altitude for the background fit, Since the signal-induced noise problem is sensitive to parameters such as laser power, low altitude haze and aerosols, and alignment of laser and telescope, there was no uniform way to handle the adjustment. The GSFC revised data therefore terminated the profile, so as to avoid a subjective approach that would have “tuned” their profile toward the average. The only permanent solution to the problem appears to be the installation of a shutter device to physically block the low altitude scattering,

As discussed earlier, the JPL lidar team used a fixed starting point (85 km) for the background retrieval, and occasionally truncated their retrieved ozone profile at 47 km instead of 50 km when there was evidence of interference from, for example, clouds.

Figure 9 shows the comparison of the Brewer Umkehr retrieved profile to the STOIC Reference. Agreement is within 15% over the 20-45 km region and 5% between 30-40 km, as discussed in greater detail in McElroy and Kerr (this *issue*). The performance of the Dobson Umkehr relative to ECC sondes is described in Komhyr et al. (this *issue*).

Ground-based direct sun measurements of total ozone were made by the Brewer spectrophotometer at frequent intervals throughout each day and by the Dobson spectrophotometer several times each morning and afternoon during STOIC. The Brewer measured daily average ozone values for all days between July 19 and August 2 are given in Figure 10. The average total ozone over the 15 day period was 297.8 DU with a standard deviation of ± 4 DU. A systematic diurnal variation of total ozone was observed throughout the period, with ozone values in the late afternoon averaging 6.6 ± 0.7 DU larger than the morning. This variability can be attributed to the build-up of low-level ozone during the day (see McDermid and Walsh, this *issue*). Results of 26 morning and afternoon Brewer and Dobson total ozone comparisons indicated that the Dobson instrument measured 1.2 DU (0.4%) less ozone than did the Brewer instrument. A comparison of Brewer column ozone to that obtained by TOMS shows TOMS values about 4.6% larger, substantially different from past comparisons, possibly resulting from the high altitude of the TMF site versus the normal tropospheric correction used by TOMS. Detailed discussion of the total ozone results and comparisons with other measurements are presented in Kerr and McElroy (this *issue*).

CONCLUSION

The STOIC results provide a demonstration that the instruments newly developed for the NDSC have the capability of producing highly

accurate and intercomparable measurements of the ozone vertical abundance, approaching 5% accuracy over the 20-40 km range. Periodic "blind" comparisons such as this have value not only for establishing the credibility of various techniques, but also for identifying possible improvements to instruments, algorithms, and procedures. Such campaigns should be an integral part of ongoing measurement systems, including ground-based, balloon, aircraft, and space-based sensors.

ACKNOWLEDGMENTS

An effort such as STOIC obviously requires the cooperation of a large number of people, institutions and agencies. Many of them are identified in the individual papers of this collection, and are implicitly included here. Funding for the STOIC participants was provided by a number of sources, including NASA, NOAA, and AES/Canada. The help and cooperation of the staff of TMF and of the Navy at Pt. Mugu and San Nicholas Island were essential to our success. A portion of the work described in this paper was carried out by the Jet Propulsion Laboratory, California Institute of Technology, under a contract with the National Aeronautics and Space Administration.

STOIC PAPERS IN THIS ISSUE

Barnes, R. A., C. L. Parsons, and A. P. Grothouse, ROCOZ-A Ozone Measurements During the Stratospheric Ozone Intercomparison Campaign (STOIC)

Barnes, R. A., A. L. Torres, Electrochemical Concentration Cell Ozone Soundings at Two Sites During the STOIC Campaign

Connor, B. J., A. Parrish, J. J. Tsou, and M. P. McCormick, Error Analysis for the Ground-based Microwave Ozone Measurements During STOIC

Ferrare, R. A., T. J. McGee, D. Whiteman, J. Burris, M. Owens, J. Butler, R. A. Barnes, F. Schmidlin, W. Komhyr, P. H. Wang, M. P. McCormick, and A. J. Miller, Lidar Measurements of Stratospheric Temperature During STOIC

Kerr, J. B. and C. T. McElroy, Total Ozone Measurements made with the Brewer Ozone Spectrophotometer during STOIC 1989

Komhyr, W. D., J. A. Lathrop, D. P. Opperman, R. A. Barnes, and G. B. Brothers, ECC Ozonesonde Performance Evaluation During STOIC 1989

Komhyr, W. D., B. J. Connor, I. S. McDermid, T. J. McGee, A. D. Parrish, and J. J. Margitan, Comparison of STOIC 1989 Ground-based Lidar, Microwave Spectrometer, and Dobson Spectrophotometer Umkehr Ozone Profiles with Ozone Profiles from Balloon Borne ECC Ozonesondes

McDermid, I. S., S. Godin, and T. D. Walsh, Results from the JPL Stratospheric Ozone Lidar During STOIC 1989

McDermid, I. S. and T. D. Walsh, Surface Ozone Levels at Table Mountain During STOIC 1989

McGee, T. J., R. Ferrare, D. Whiteman, J. Butler, J. Burris, and M. Owens, Lidar Measurements of Stratospheric Ozone During the STOIC Campaign

McElroy, C. T., and J. B. Kerr, Table Mountain Ozone Intercomparison: Brewer Ozone Spectrophotometer Umkehr Observations

REFERENCES

- Barnes, R. A., M. A. Chamberlain, C. L. Parsons, and A. C. Holland, An Improved Rocket Ozonesonde (ROCOZ-A) 3. Northern Mid-Latitude Ozone Measurements from 1983 to 1985, *J. Geophys. Res.* 94, 2239-2254, 1989
- Bass, A. M, and R. J. Paur, The ultraviolet cross-sections of ozone: 1. The Measurements, in *Atmospheric Ozone, Proc. Quadrennial Ozone Symposium*, Halkidiki, Greece, September 3-7, 1984, ed. by C. S. Zerefos and A. Ghazi, 606-610, D. Reidel, Dordrecht, Holland, 1985
- Evans, W, F. J., H, Fast, A. J. Forester, G. S. Henderson, J. B. Kerr, R, K. R. Vupputuri and D. I. Wardle, Stratospheric ozone science in Canada: An agenda for research and monitoring, *Internal Rep. ARD-87-3*, Environment Canada, 1987
- Gotz, F. W. P., A. R. Meetham, and G. B. B. Dobson, The vertical distribution of ozone in the atmosphere, *Proc. Roy. Soc., London*, A145, 416, 1934
- Hilsenrath, E., W. Attmannspacher, A. Bass, W. Evans, R. Hagemeyer, R. A. Barnes, W. Komhyr, K. Mauersberger, J. Mentall, M. Proffitt, D. Robbins, S. Taylor, A. Torres, and E. Weinstock, Results from the Balloon Ozone Intercomparison Campaign (BOIC), *J. Geophys. Res.* 91, 13137-13152, 1986
- Iikura, Y., N. Sugimoto, Y. Sasano, and H. Shimizu, Improvement on lidar data processing for stratospheric aerosol measurements, *Appl. Opt.*, 26, 5299-5306, 1987
- Kerr, J. B., C. T. McElroy and W, F. J. Evans, The automated Brewer spectrophotometer for measurement of SO₂, O₃, and aerosols, *Proc. WMO/AMS/CMOS Symposium on Meteor, Observations and Instrumentation*, Toronto, 470-472, 1983
- Kerr, J. B., C. T. McElroy, D. I. Wardle, R. A. Olafson and W. F. J. Evans, The automated Brewer spectrophotometer, in *Atmospheric Ozone, Proc. Quadrennial Ozone Symposium*, Halkidiki, Greece, ed. by C. S. Zerefos and A. Ghazi, D. Reidel, Hingham, MA, 396-401, 1985
- Komhyr, W. D., R. D. Grass and R. K. Leonard, Dobson spectrometer 83: A standard for total ozone measurements, *J. Geophys. Res.* 94, 9847-9861, 1989
- Komhyr, W. D., C. L. Mateer and R. D. Hudson, Effective Bass-Paur 1985 ozone absorption coefficients for use with Dobson ozone spectrophotometers, *J. Geophys. Res.* 98, 20451-20466, 1993

- Lee, H. S., G. K. Schwemmer, C. L. Korb, M. Dombrowski, and C. Prasad, Gated photomultiplier response characterization for DIAL measurements, *Appl. Opt.*, 29,3303-3315,1990,
- Mateer, C. L., and H. U. Dutsch, Uniform evaluation of Umkehr observations from the World Ozone Network, Part I. Proposed standard evaluation technique, 105 pp, National Center for Atmospheric Research, Boulder, CO, 1964
- Mateer, C. L., J. B. Kerr and W. F. J. Evans, Ozone profiles derived from Umkehr observations obtained with the Brewer ozone spectrophotometer, in *Atmospheric Ozone, Proc. Quadrennial Ozone Symposium*, Halkidiki, Greece, ed. by C. S. Zerefos and A. Ghazi, D. Reidel, Hingham, MA, 407-411, 1985
- Mateer, C. L., and J. J. DeLuisi, A new Umkehr inversion algorithm, *J. Atmos. and Terrestrial Physics*, 54, 537-556, 1992
- McDermid, I. S., and S. M. Godin, Stratospheric Ozone Measurements Using a Ground-Based, High-Power Lidar, *Laser Applications in Meteorology and earth and Atmospheric Remote Sensing*, edited by M. M. Sokolowski, *Proc. SPIE Int. Soc. Opt. Eng.*, 1062,225-232,1989.
- McDermid, I. S., S. M. Godin, and L. O. Lindqvist, Ground-Based Laser DIAL System for Long-Term Measurements of Stratospheric Ozone, *Appl. Opt.*, 29,3603-3612, 1990a.
- McDermid, I. S., S. M. Godin, and T. D. Walsh, Lidar Measurements of Stratospheric Ozone and Intercomparisons and Validation, *Appl. Opt.*, 29, 4914-4923, 1990b.
- McElroy, C. T. and J. B. Kerr, Table Mountain ozone intercomparison: Brewer ozone spectrophotometer Umkehr observations, *Proc. of Optical Remote Sensing of the Atmosphere Topical Meeting*, Incline Village, NV, 445-448, 1990
- McElroy, C. T., C. L. Mateer, J. B. Kerr and D. 1. Wardle, Umkehr observations made with the Brewer ozone spectrophotometer, *Ozone in the Atmosphere*, Proc. Quadrennial Ozone Symposium, Gottingen, FRG, 725-727,1989
- McGee, T. J., D. Whiteman, R. Ferrare, J. J. Butler and J. Burris, STROZ LITE: Stratospheric Ozone Lidar Trailer Experiment, *Opt. Eng.*, 30,31-39, 1991
- Parrish, A., B. J. Connor, J. J. Tsou, I. S. McDermid, and W. P. Chu, Ground based microwave monitoring of stratospheric ozone, *J. Geophys. Res.*, 97, 2541-2546,1992

Rodgers, C. D., Retrieval of Atmospheric Temperature and Composition From Remote Measurements of Thermal Radiation, *Rev. of Geophys. and Space Phys.*, 14,609-624, 1976.

Vigroux, E., Contribution a l'etude experimentale de l'absorption de l'ozone, *Ann, Phys.*, 8,709-762, 1953

Vigroux, E., Determination des coefficients moyens d'absorption de l'ozone en vue des observations concernant l'ozone atmosferic a l'aide du spectrometre Dobson, *Ann. Phys.*, 22, 209-215, 1967

WMO Report No. 16, *Atmospheric Ozone 1985, Assessment of our understanding of the processes controlling its present distribution and change*, World Meteorological Organization, Global Ozone Research and Monitoring Project-Report No. 16, avail. NASA, Washington, DC, 1985

WMO Report No. 18, *Report of the international Ozone Trends Panel 1988* World Meteorological Organization, Global Ozone Research and Monitoring Project-Report No. 18, avail. NASA, Washington, DC, 1988

WMO Report No. 25, *Scientific Assessment of Ozone Depletion: 1991*, World Meteorological Organization, Global Ozone Research and Monitoring Project-Report No. 25, avail. NASA, Washington, DC, 1991

Table 1. Stratospheric Ozone Intercomparison Campaign

Investigator	Institution	Instrument	Alt.km	Lot.	PDT Obs. Time, hrs
I. S. McDermid	JPL	Lidar (JL)	20-50	TMF	22-24
T. McGee	GSFC	Lidar (GL)	20-45	TMF	00-05
A. Parrish/B. Connor	Millitech/LaRC	Microwave (MM)	20-64	TMF	22-05
C. Parsons/R. Barnes	WFF	ROCOZ (RO) ECC sondes (WS, MS)	20-60 0-35	SN TMF/Mu	12-15 23-01
W. D. Komhyr	NOAA	Dobson Umkehr/Dobson ECC sondes (NS)	column 0-50 0-40	TMF TMF TMF	07-19 SR,SS 23-02
J. Kerr/T. McElroy	AES/Canada	Brewer Umkehr/Brewer	column 0-50	TMF TMF	07-19 SR,SS
M. P. McCormick	Langley	SAGE II (SA)	10-60	Sat.	SR
A. J. Krueger	GSFC	TOMS	column	Sat _s	noon
A. J. Miller	NOAA	Met. data		Sat.	

2-letter codes in parenthesis in instrument column are used to identify data in the Figures

TMF Table Mountain Facility

SN San Nicholas Island
 Mu Pt. Mugu
 Sat. Satellite measurement
 SR sunrise
 SS sunset

Table 2. STOIC Observations

Date	JL	GL	MM	WS	NS	RO	SA	MS
890720	X	x	X	X		X		x
890721	X	x	x	x	x			x
890722	X		x	x				x
890723	X	x	x	x	x		x	
890724	X	x	x	x	x	X	x	X
890725	X	x	x	x	x		x	X
890726	X	x	x	x	x	X		X
890727	X	x	x	x	x	X		X
890728	X		x			X		X
890729	X	x	x	X				X
890730	X	x	x	X	X			X
890731	X	x	x	X	X			X
890801	X	x	x	X	X			X
890802	X	x	x	X	X	X		X
# Ohs.	14	12	14	13	10	6	3	13

Table3 Precision, Accuracy, and Range Resolution

Alt		JL	GL	MM	WS	NS	RO	SA	Umkehr
50	P	5-25	10-15	5			5	5	
	A	10-50	20-30	9			7	8	
	R	8	@45km	1 4			4	5	
40	P	2-5	5	5		10	3.5	5	5
	A	4-10	10	8		20	7	8	12
	R	4	5	10		0.5	4	1	12
30	P	1	1	4	6	3	3.5	5	5
	A	2	2	6	10	5	7	8	12
	R	1	2.5	8	0.3	0.5	4	1	14
20	P	1	1	4	6	3	5	5	8
	A	2	2	7	10	5	7	8	12
	R	1	1	10	0.3	0.5	4	1	13

P=precision (%)

A=accuracy (%)

R=range resolution (km)

The individual instrument papers should be consulted for the origin and exact meaning of these parameters. They may not be strictly comparable among the very different techniques in use here.

FIGURE CAPTIONS

FIGURE 1. Altitude ranges for the STOIC instruments, showing where data were reported on more than 50% of the observations, and less than 50% of the observations. Note, for example, that SAGE shows full coverage, although there were only 3 SAGE observations in this period: all of them had data over the whole range. On the other hand, GL had 12 observations, but not all of them covered their whole altitude range.

FIGURE 2. Ozone data for July 24, 1989. "Blind" data from all instruments. (a) linear ozone scale; (b) logarithmic ozone scale.

FIGURE 3. Ozone data for July 24, 1989. "Revised" data from all instruments. (Compare to Fig. 2). (a) linear ozone scale; (b) logarithmic ozone scale.

FIGURE 4. Daily average profiles over the campaign, showing the degree of day-to-day variability in ozone that occurred. (a) First 7 days, linear scale; (b) First 7 days, log scale; (c) Second 7 days, linear scale; (d) Second 7 days, log scale.

FIGURE 5. STOIC ozone variability shown as a contour plot over the 14 day period. Note that there was little day-to-day variability except near the peak, where it was about 10%.

FIGURE 6. "Blind" instrument averages over the period. (a) linear scale (b) log scale

FIGURE 7. (a) Comparison of "Blind" instrument averages to the STOIC Reference Profile (see text). Plotted as $((\text{Instrument}/\text{Reference}) - 1)$; i. e., 0.1 is an instrument that was 10% above the reference. (b) Similar to (a) but for the "Revised" data. The STOIC Reference is the same for both plots, so that changes are due solely to revisions to the instrument data, not the reference.

FIGURE 8. Standard deviations of the data versus altitude, showing atmospheric variability, and the deviations in both blind and revised instrument profiles.

FIGURE 9. Comparison of the Brewer Umkehr profile to the mean of the other STOIC data.

FIGURE 10. Comparison of total ozone column measured by the Brewer and by TOMS.

ALTITUDE RANGE FOR STOIC INSTRUMENTS

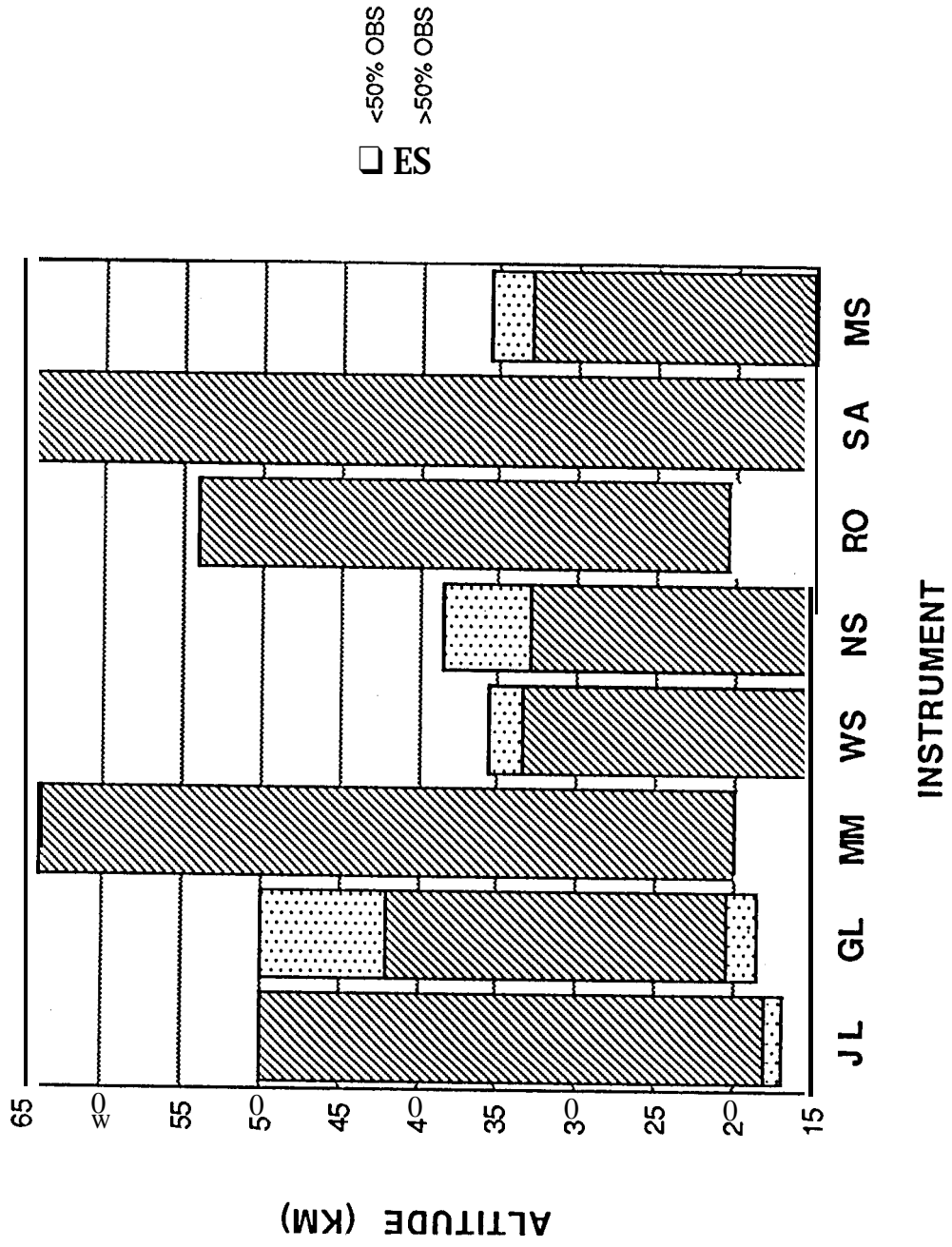


Figure 1

890724 BLIND DATA

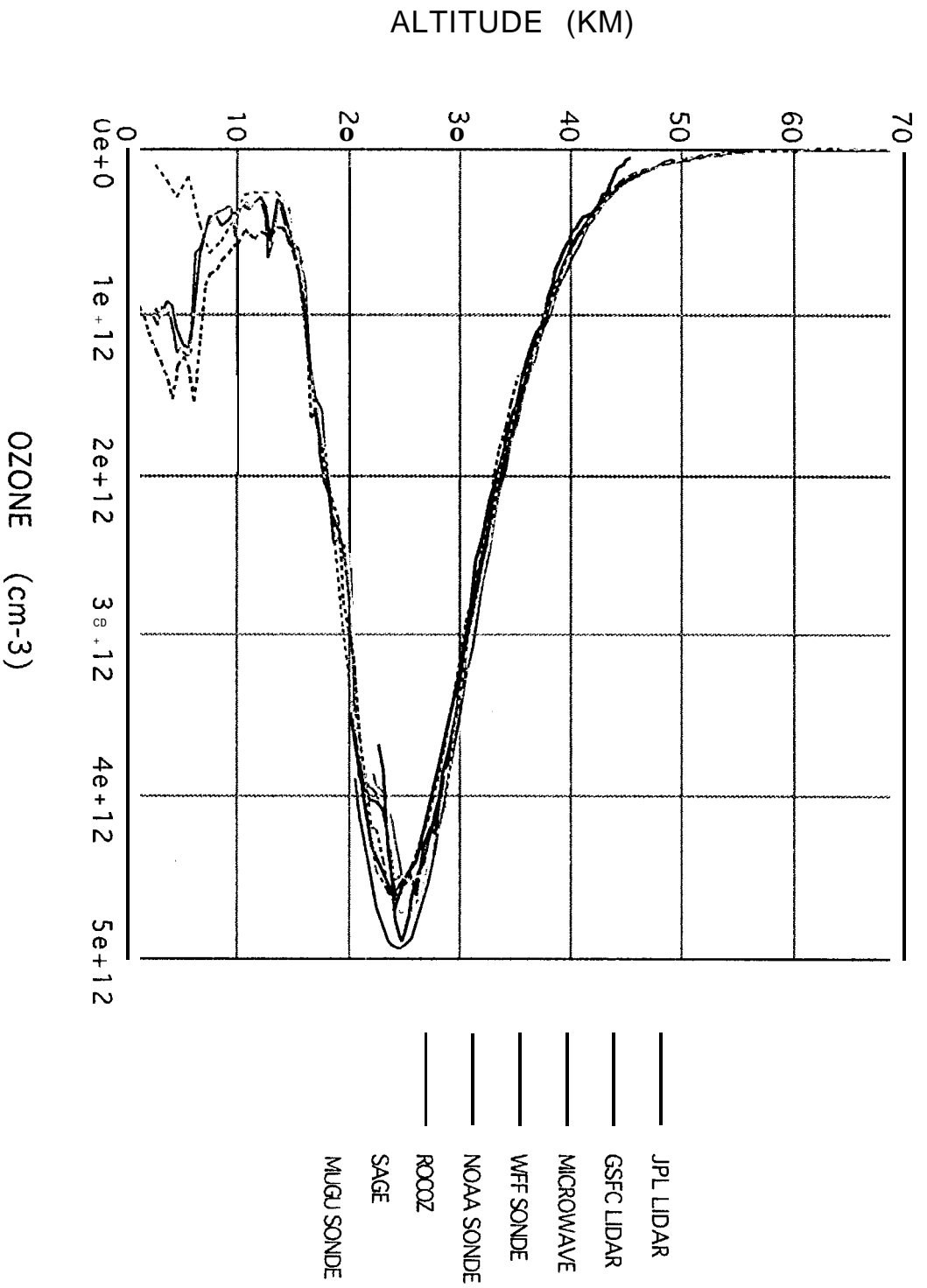


Figure 2a

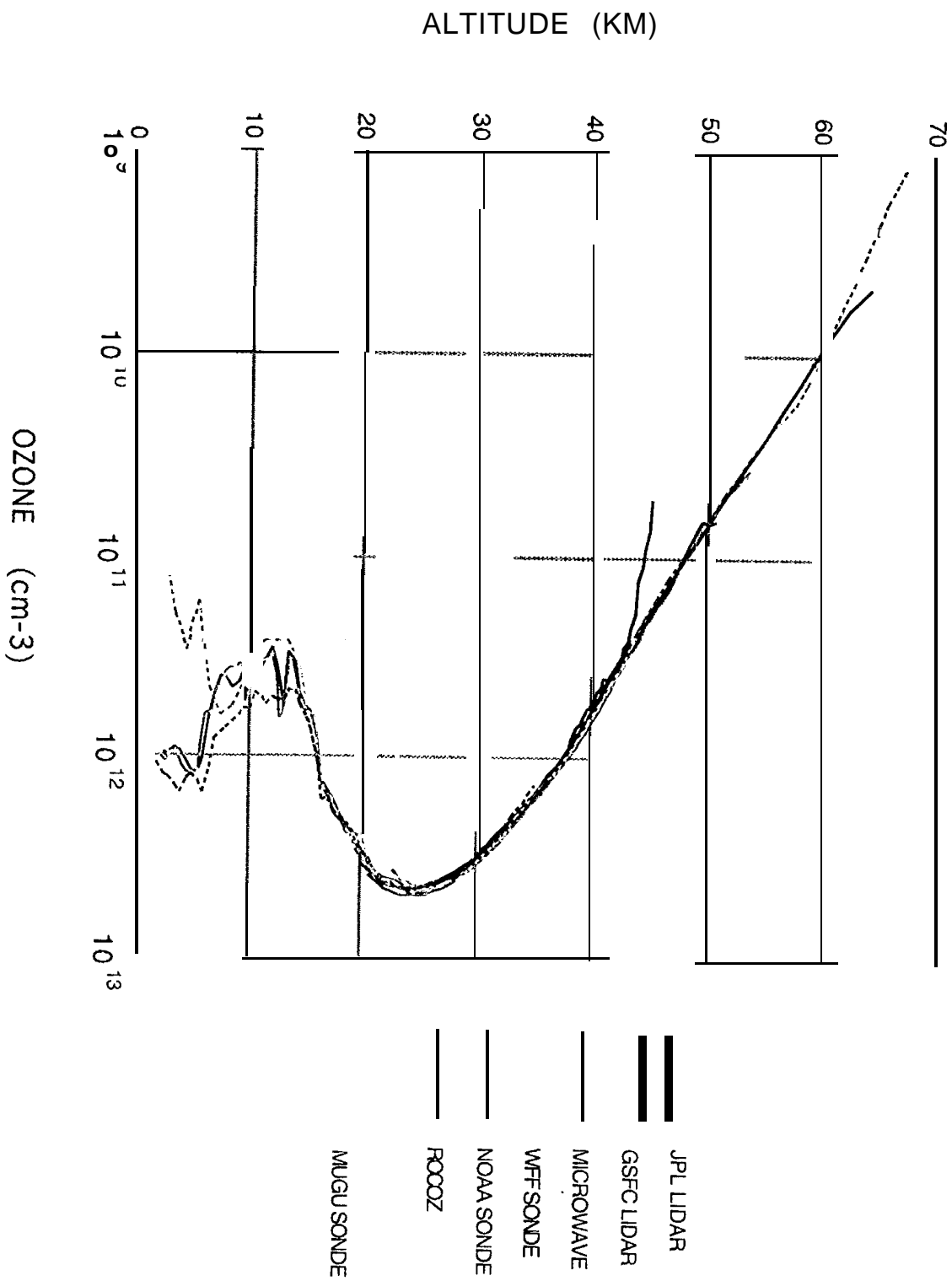


Figure 2b

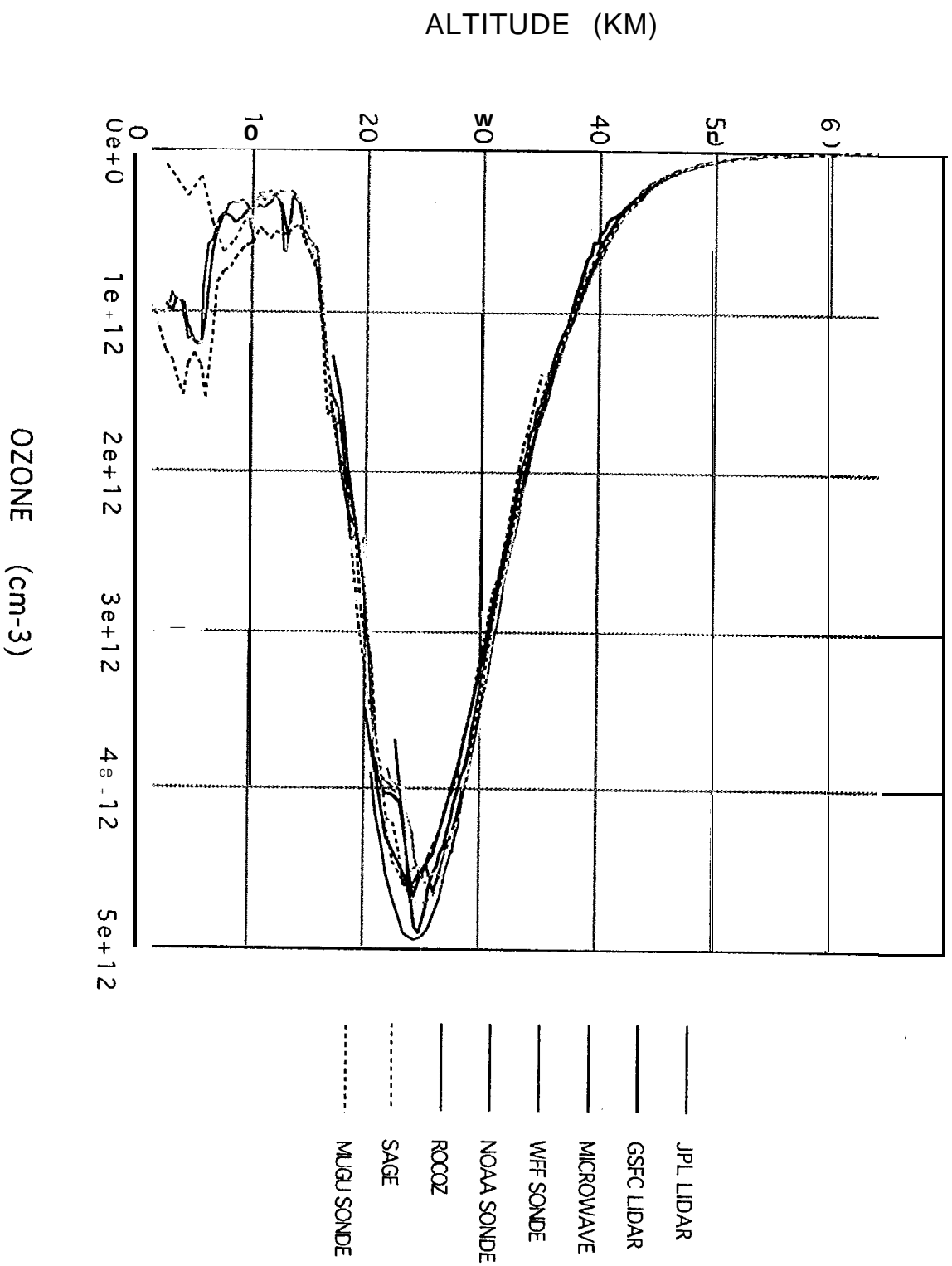


Figure 3a

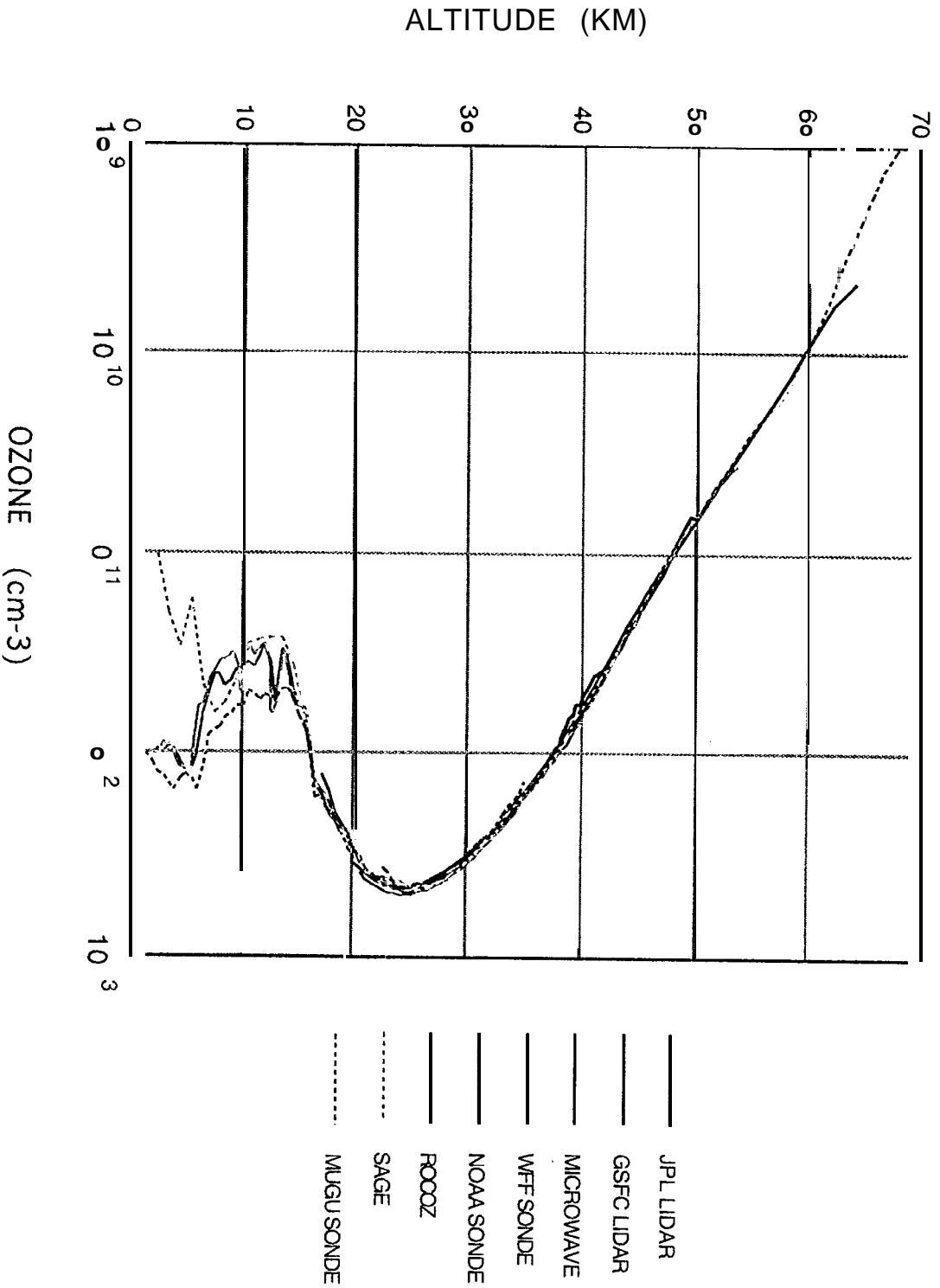


Figure 3b

DAILY AVERAGE PROFILES

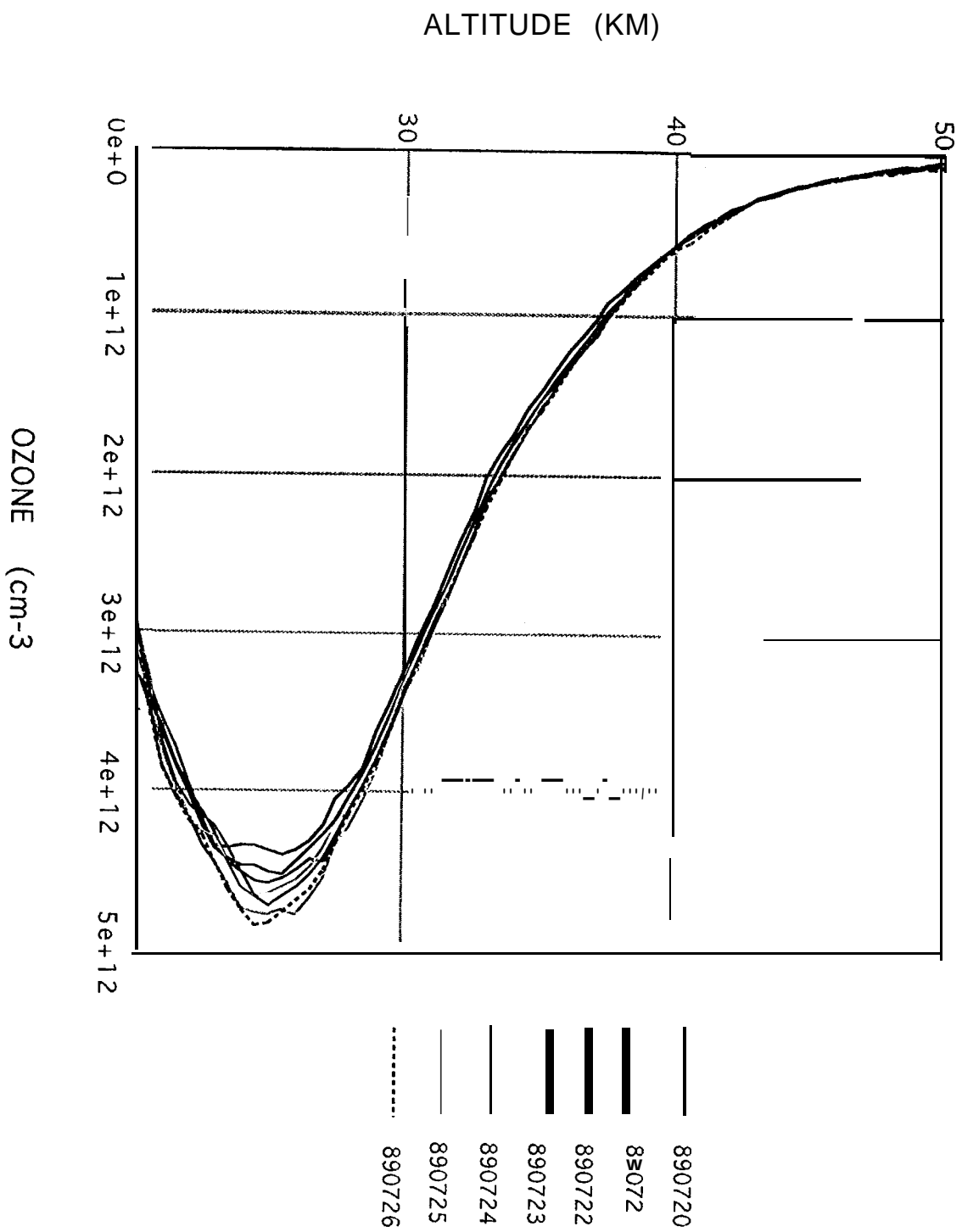


Figure 4a

DAILY AVERAGE PROFILES

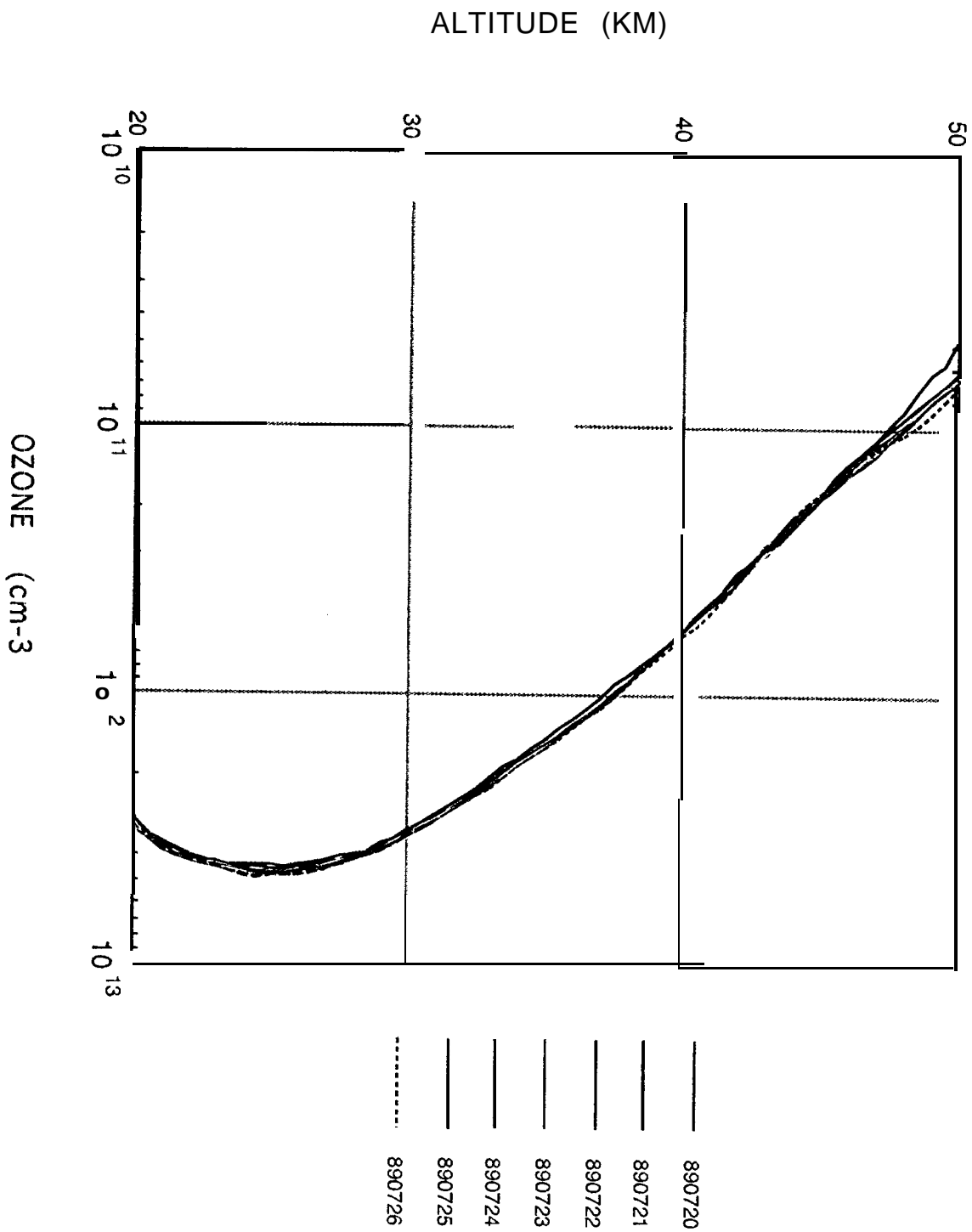
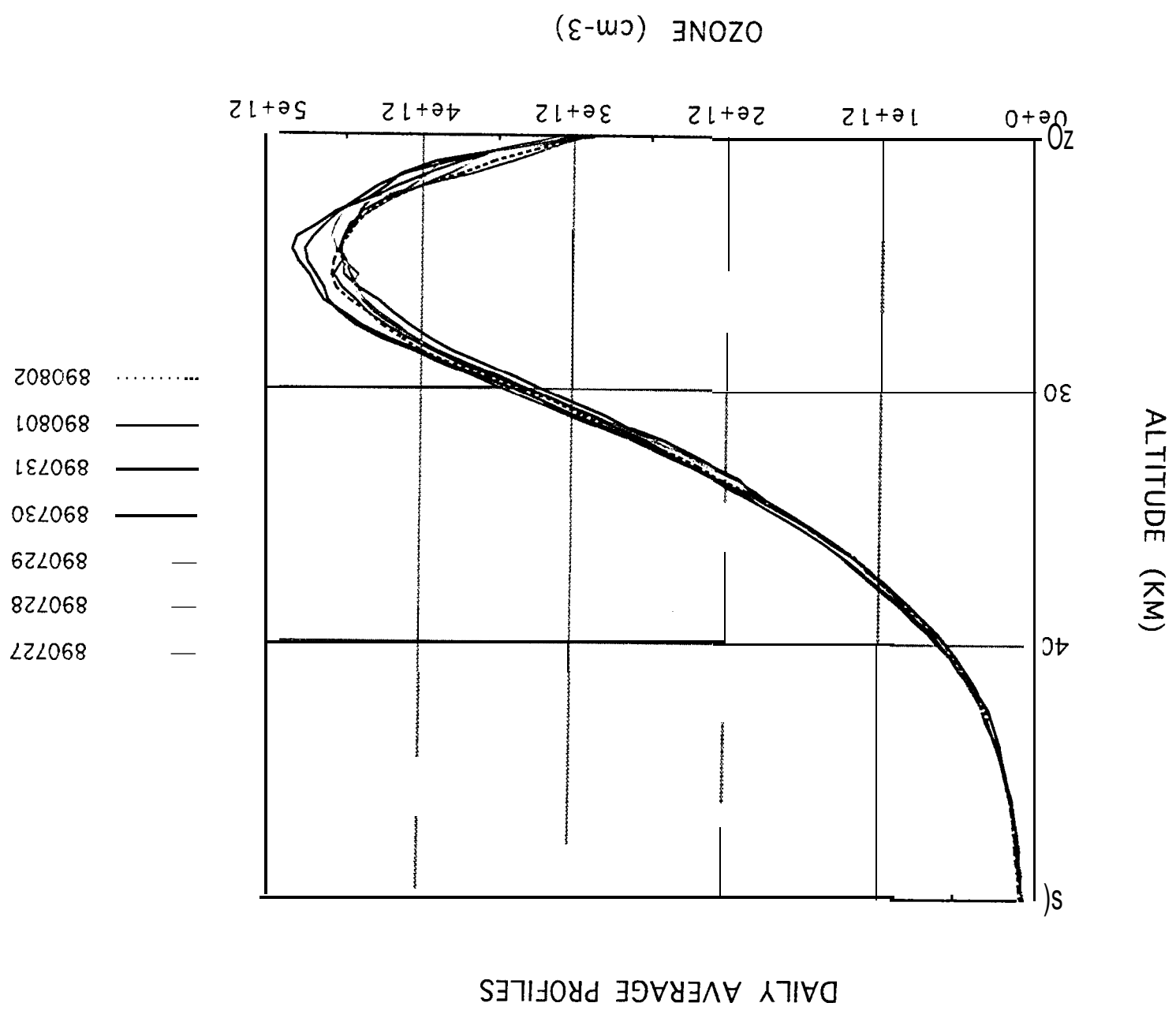
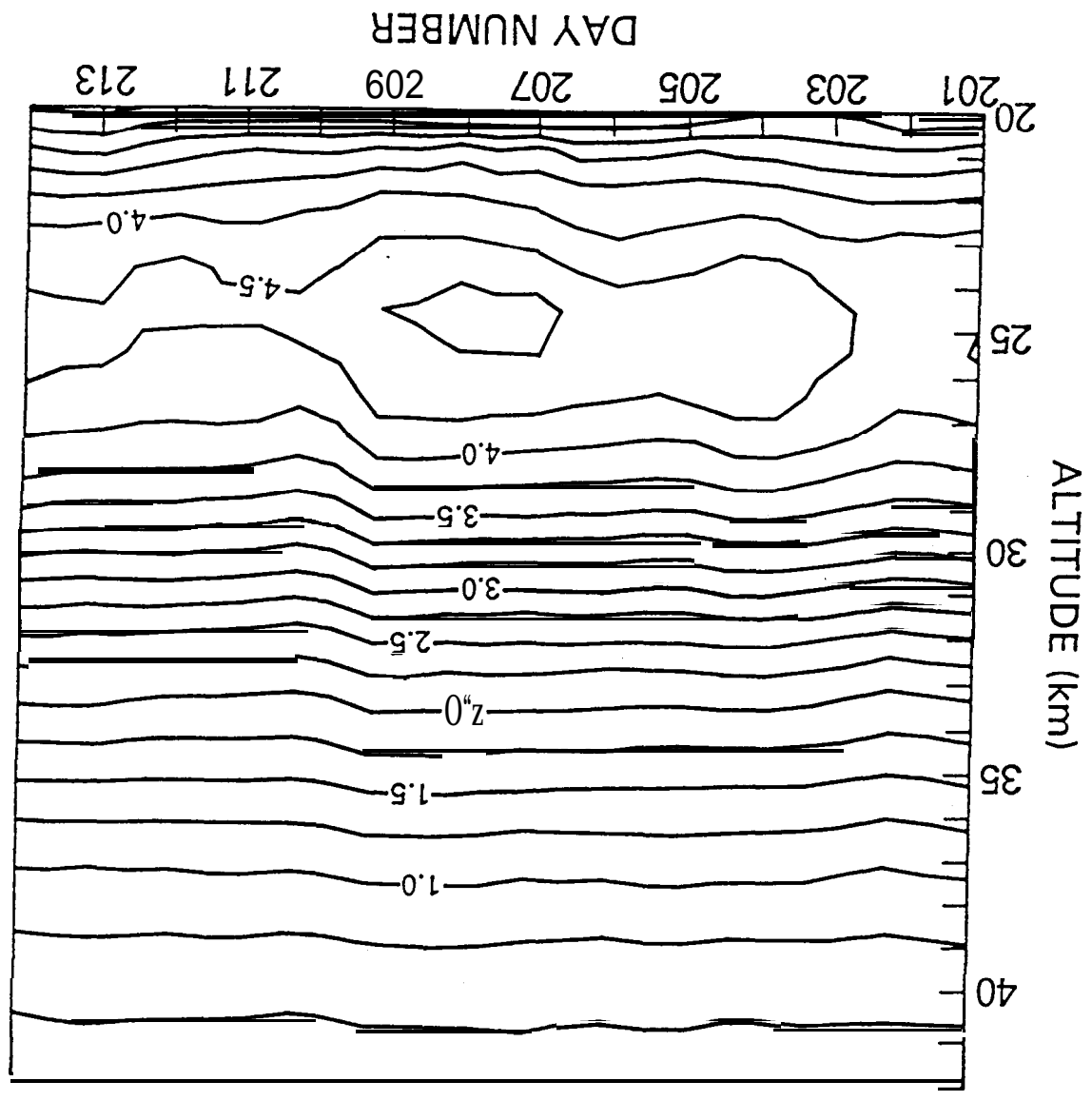


Figure 4b





STOIC OZONE RESULTS
OZONE NUMBER DENSITY ($\times 10^{12}$ molecules/cm³)

STOIC INSTRUMENT AVERAGES -- BLIND DATA

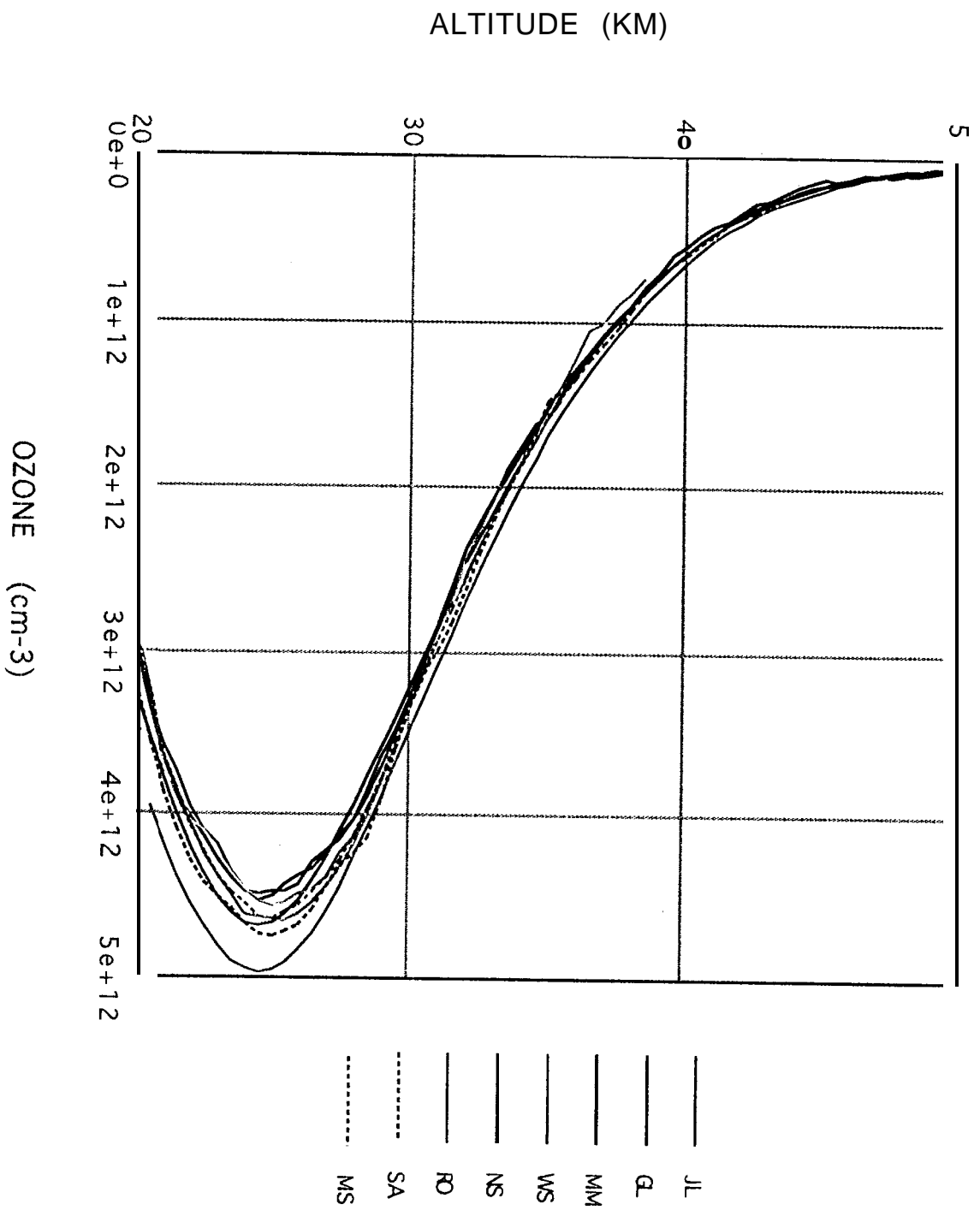


Figure 6a

STOIC INSTRUMENT AVERAGES -- BLIND DATA

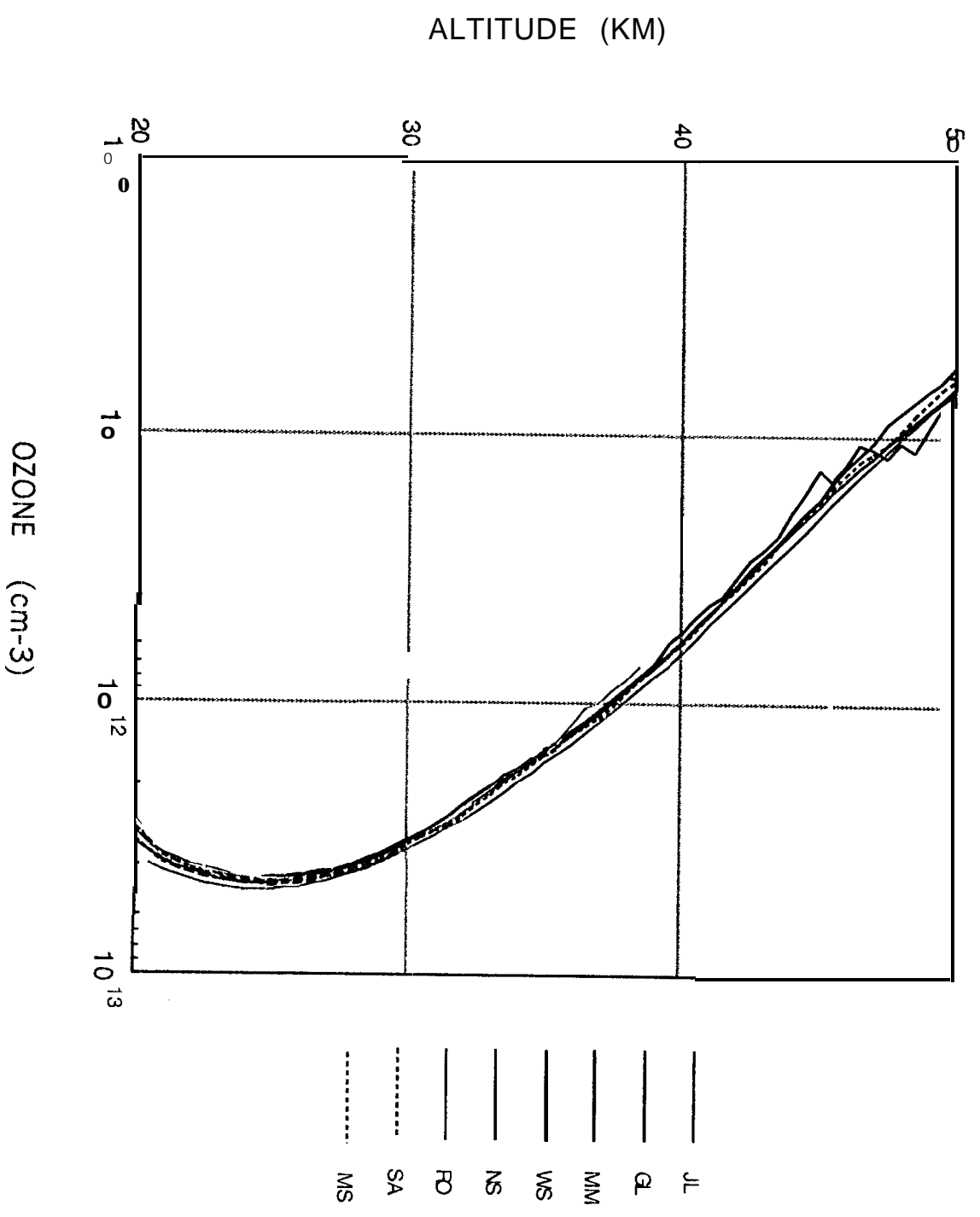


Figure 6b

COMPARISON OF INSTRUMENT AVERAGES TO REFERENCE PROFILE
(blind data)

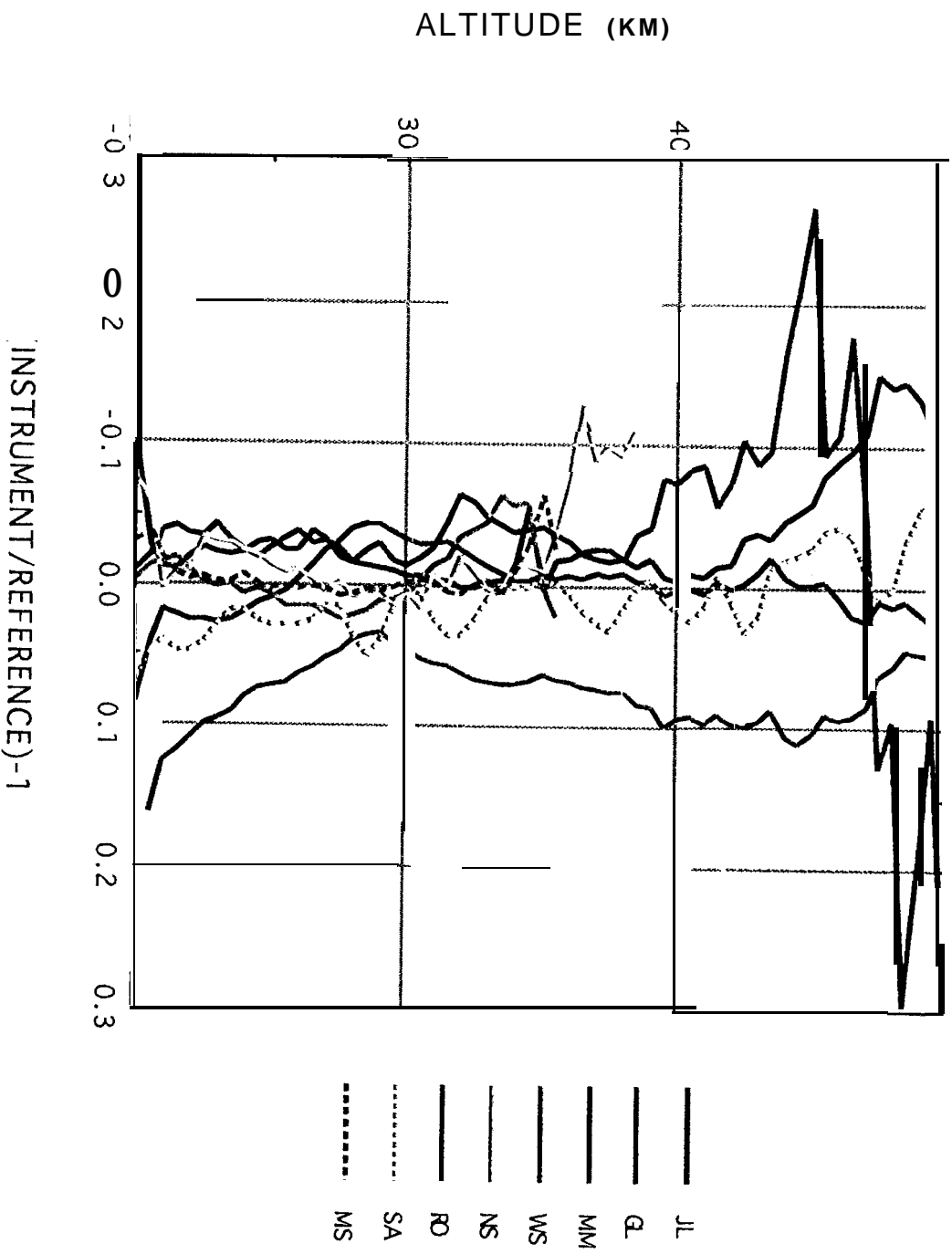


Figure 7a

COMPARISON OF INSTRUMENT AVERAGES TO REFERENCE PROFILE
(revised data)

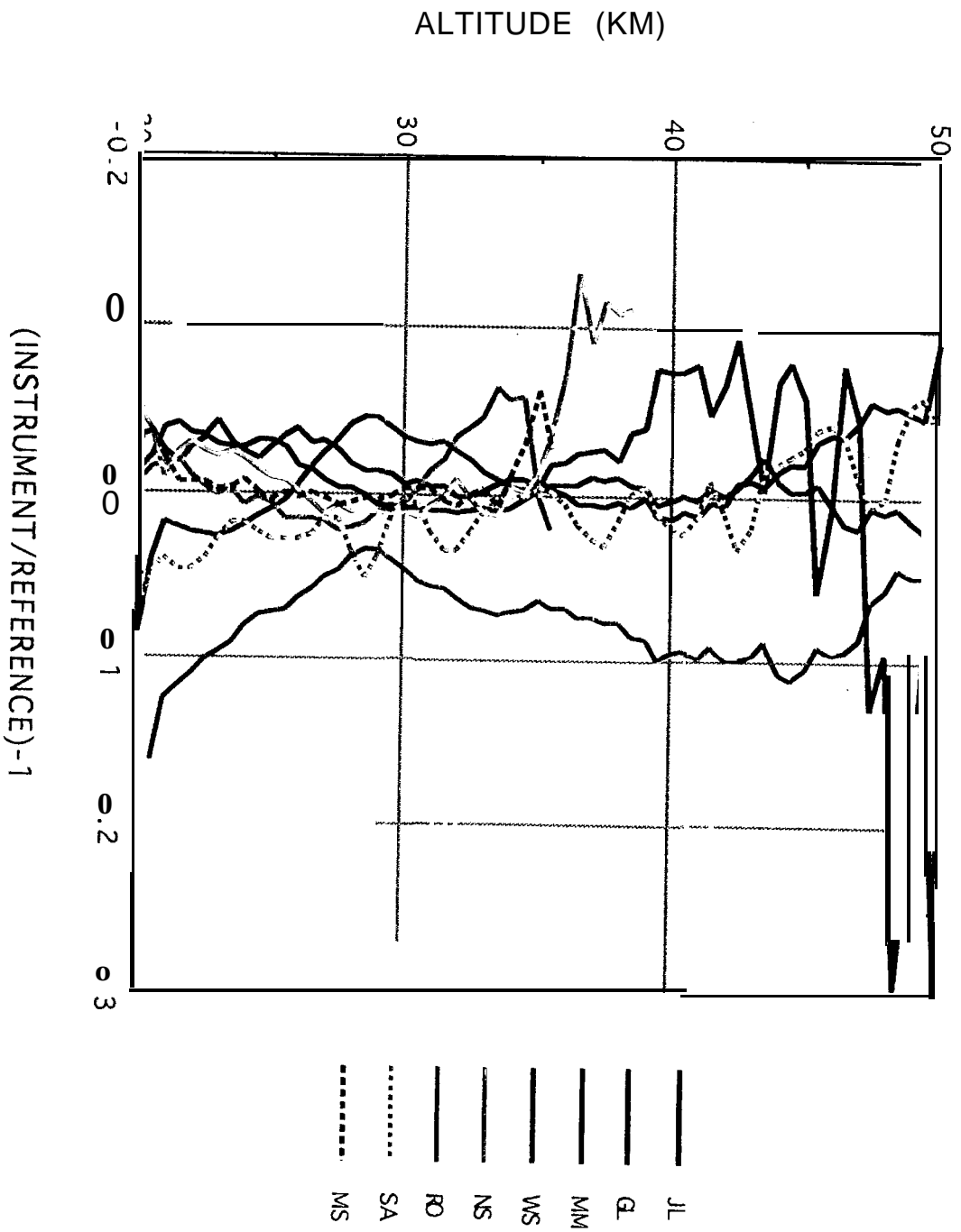
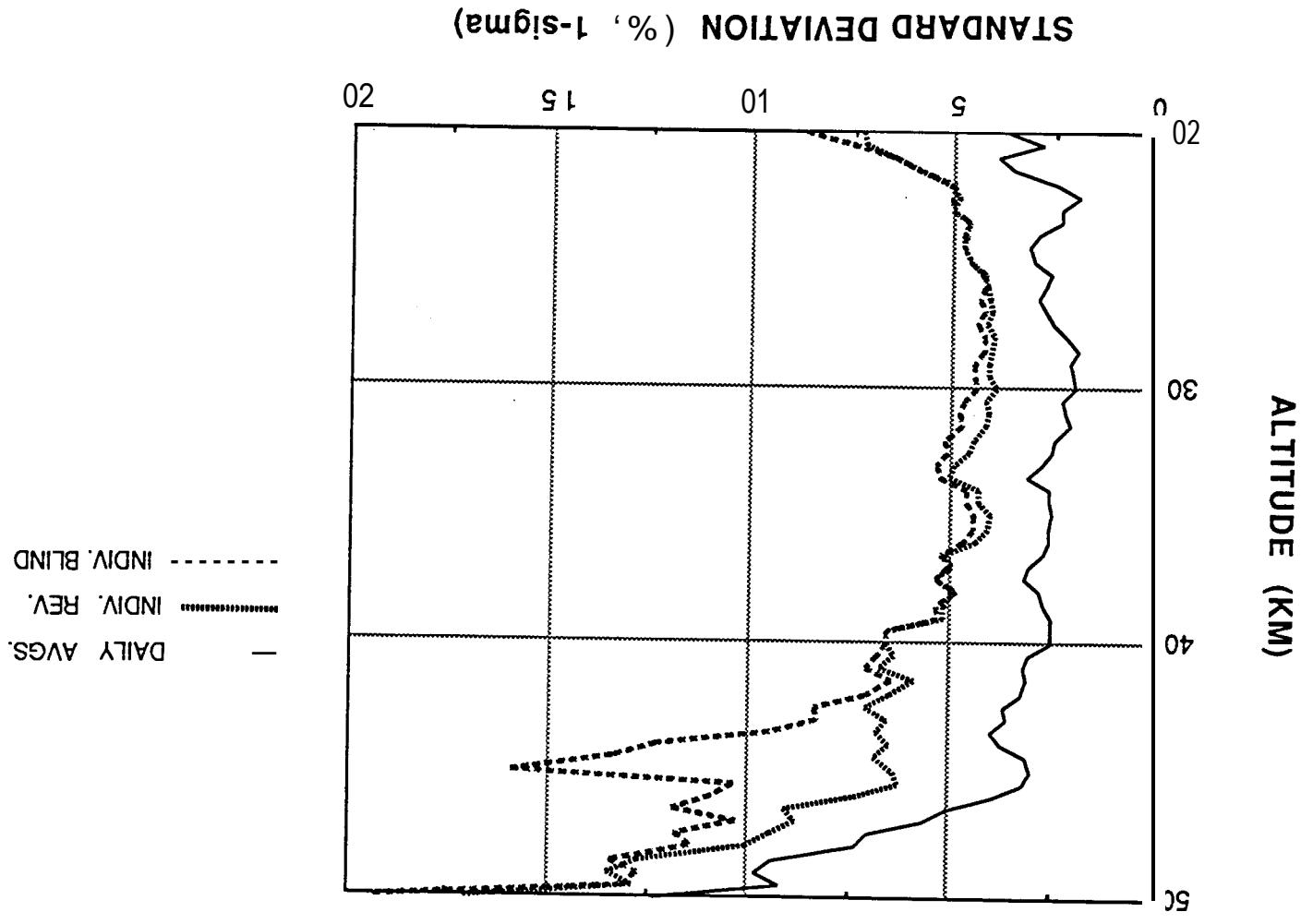


Figure 7b



STANDARD DEVIATIONS FROM AVERAGING PROFILES:
DAILY AVGS., ALL INDIVIDUAL (REVISED), ALL INDIVIDUAL (BLIND)

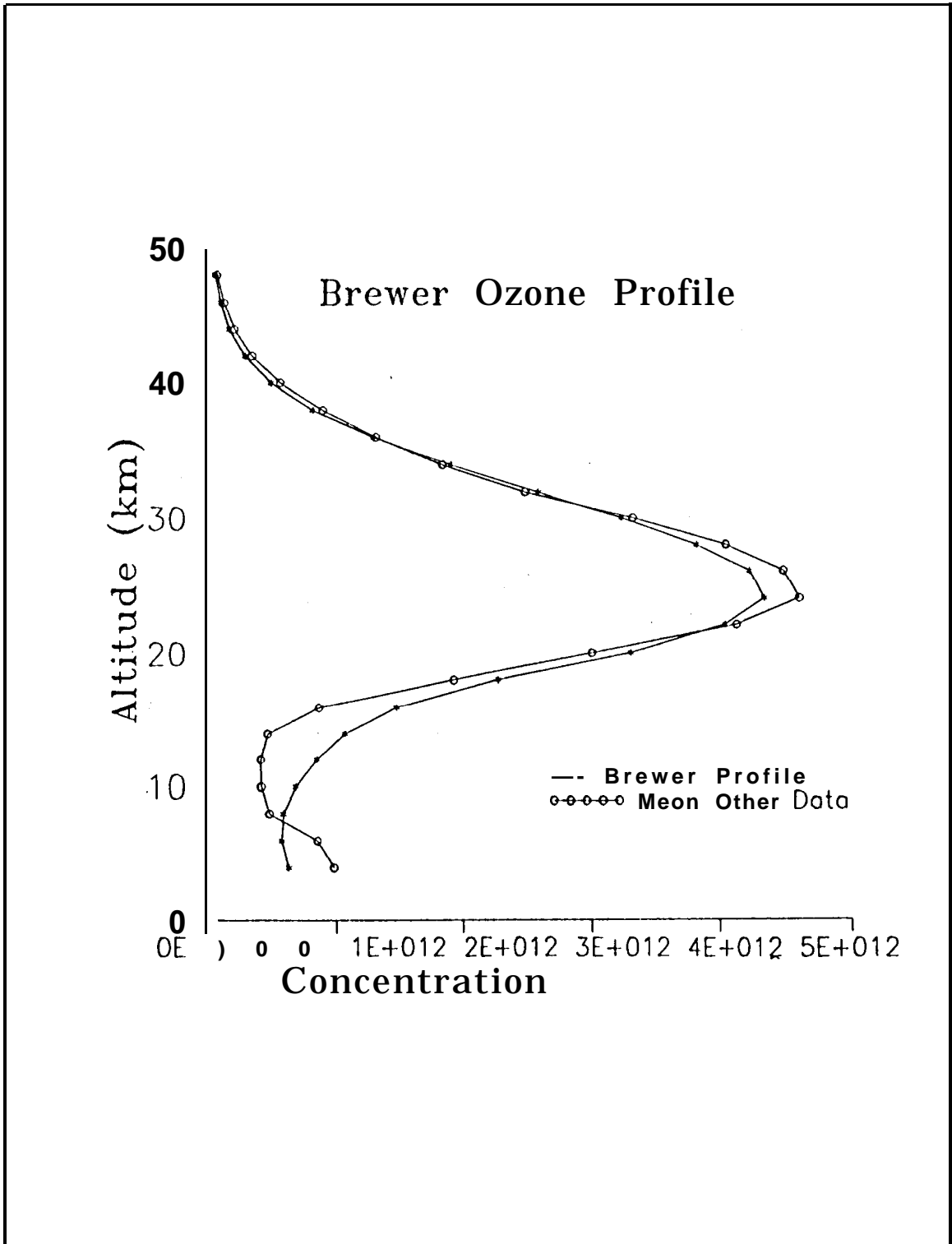


Figure 9

LOCAL NOON TOTAL OZONE

TOTAL OZONE (DU)

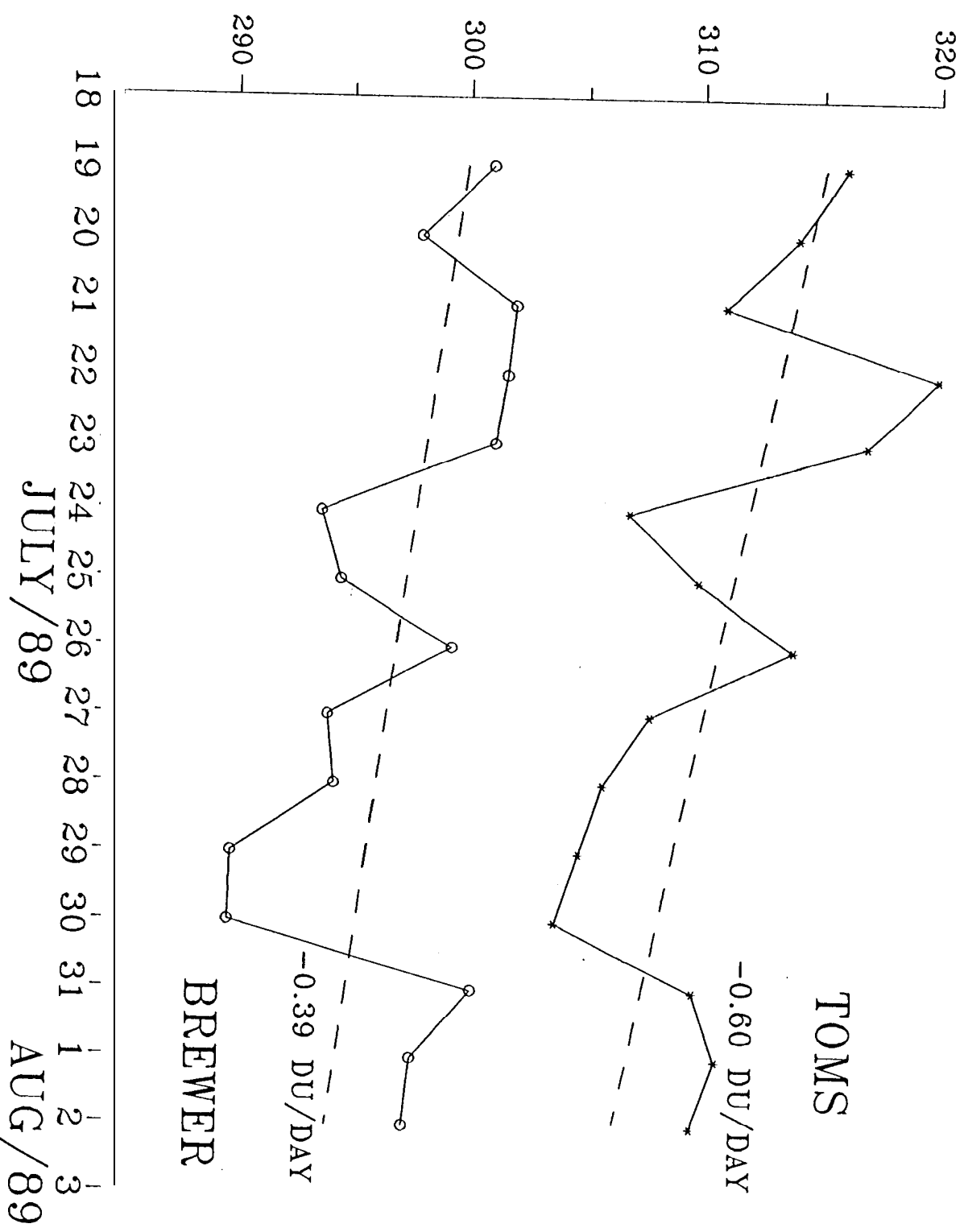


Figure 10